

Effect of Mixing Temperature, Ultrasonication Duration and Nanoparticles/Surfactant Concentration on the Dispersion Performance of Al₂O₃ Nanolubricants

Haijun Liu

Wuhan University of Technology

Xianjun Hou (✉ houxj@whut.edu.cn)

Wuhan University of Technology

Xiaoxue Li

Ordos Institute of Technology

Hua Jiang

Wuhan University of Technology

Zekun Tian

Wuhan University of Technology

Mohamed Kamal Ahmed Ali

Wuhan University of Technology

Nano Express

Keywords: Aluminium oxide, Nanolubricant, Dispersion stability, Dispersion mechanism, Ultrasonication duration, Absorbancy

Posted Date: October 5th, 2020

DOI: <https://doi.org/10.21203/rs.3.rs-84466/v1>

License:  This work is licensed under a Creative Commons Attribution 4.0 International License.

[Read Full License](#)

Abstract

The main goal of this study is to improve the dispersion stability of Al₂O₃ nanoparticles in polyalphaolefin oil to overcome the sedimentation problem of nanoparticles using the addition of oleic acid as a surfactant. This work investigates the effect of the settling time, temperature, ultrasonic duration and nanoparticles/surfactant (oleic acid) concentration on the dispersion stability of Al₂O₃ nanoparticles in oil-based solutions. Herein, the visual observation, UV–Vis spectroscopy, dynamic light scattering (DLS) analysis, and transmission electron microscopy (TEM) images were used to evaluate the dispersion stability of the Al₂O₃ nanoparticles. The results reveal that the thermal method during the synthesis of nanofluids using 50 °C temperature improves the dispersion of nanoparticles. The results also exhibited that increasing the ultrasonic amplitude and prolonging the ultrasonic time during the synthesis of nanofluids influences the dispersion stability. The results showed that the nanolubricant with 0.8 wt.% oleic acid provides better dispersion behavior. Furthermore, the nanolubricants containing 0.005wt% and 0.01wt% Al₂O₃ nanoparticles demonstrated outstanding dispersion performance, and the stability time reached more than 160 days.

Highlights

1. The dispersion stability of nanoparticles in oil has been greatly improved.
2. The stability performance of Al₂O₃ nanoparticles in oil exceeds 160 days.
3. The optimal ultrasonication amplitude and ultrasonication duration was obtained.
4. The preparation process of nanofluids was innovatively optimized.
5. Colloidal stability was characterized and evaluated by visual observation, UV, DLS, TEM.

1. Introduction

With the increasing of nanotechnology applications, nanoparticles are highly promising for improving the tribological properties, heat transfer capability, and reducing fuel consumption[1-3]. A lot of research has been done on various nanomaterials as oil-based lubricant additives to reduce friction and wear or enhanced thermal conductivity[1, 4-26]. Some researchers have also carried out research on the preparation factors of nanolubricants and the dispersion and stability of nanoparticles in various lube oils, and analyzed the failure reasons. As shown in Table 1, although nanoparticles dispersed in various oils have been proven to be effective in reducing friction, improving anti wear properties and thermal conductivity, the duration of dispersion stability is still unsatisfactory [1, 3, 22, 27-39].

Table 1
Overview of previously reported nano-particles as additives in oils:

Nanoparticles	Grain size	Concentration	Base oil	Surfactant/ dispersant	Stability time	Ref.
ZnO	20nm	0.6wt.%	10w-40	oleic acid	8days	27
rGO	60nm	0.25wt.%	PAO 40	10 days	28
CeO ₂ /CuO	50nm	0.1wt.%	coconut oil	5 days	29
Ni/MoS ₂	1um sheet	0.1wt.%	Mineral oil	10 days	30
Au/GO	4-10nm	0.1wt.%	PAO6	Oleylamine	10 days	31
ZnO	10-30nm	0.8wt.%	60SN oil	Oleic acid	0.5 days	22
Al ₂ O ₃ /TiO ₂	8-12nm	0.25wt.%	5W-30	Oleic acid	14 days	3
MoS ₂	90nm	0.53-0.58wt.%	500N Oil	SDS	5 days	32
Al ₂ O ₃	20nm	0.25wt.%	20w-40	1.5 days	33
SWCNH	97 ± 6nm	0.005wt.%	Engine oil	14 days	34
Al ₂ O ₃	78nm	0.1wt.%	Base oil	KH-560	20 days	35
TiO ₂ /Al ₂ O ₃	79nm	0.1wt.%	Mineral oil	acrylic acid	10 days	1
ZrO ₂ /SiO ₂	50-80nm	0.1wt.%	Base oil	3 days	36
Cu	40nm	0.11vol%	Gear oil	oleic acid	20 days	37
CuO	40nm	0.025vol%	Gear oil	oleic acid	30 days	38
CNC	9-14nm	0.1vol%	SAE 40	21 days	39

Among the nanoparticles in Table 1, Al₂O₃ nanoparticles, as typical inorganic nanoparticles, are widely concerned and applied due to their simple preparation and low cost. According to the research conclusion of Nishant Mohan[33], compared with base oil, The suspension containing Al₂O₃ nanoparticles showed a decrease in friction and wear under both flooded as well as starved lubrication conditions. Luo T et al[35]. confirmed that when the four-ball and wear experiment was completed with a lubricating oil containing 0.1wt % Al₂O₃. The friction coefficient and wear scar diameter are decreased effectively. Ali et al[4, 21]. studied the tribological performance for piston ring-cylinder liner contact lubricated by Al₂O₃ and TiO₂ nanolubricants, and the results showed that the hybrid nanolubricants reduced the friction coefficient and wear rate of piston rings by 39-53% and 25-33%, respectively. Moreover, the application of lubricating oil

containing Al_2O_3 nanoparticles also significantly improves the thermophysical properties. The thermal stability tests by Ali et al.[40] showed that the nanolubricants containing Al_2O_3 improved the heat transport characteristics by 9-14%. Whilst, the thermal conductivity was improved by 7–11% in the temperature ranged from 18-132°C compared with the commercial oil. In addition, Lotfizadeh et al. [41] reported that the thermal conductivity of nanofluids containing a concentration of 0.01-1.0 vol% Al_2O_3 nanoparticles improved by 4% under at 25 °C temperature.

In order to maintain long-term excellent anti-friction, rheological, and thermal conductivity properties, stable nanofluids with uniformly dispersed Al_2O_3 nanoparticles must be prepared[42]. However, nanoparticles are difficult to disperse lube oils because of the high surface energy of nanoparticles. Up to now, there is no report that nanoparticles can maintain long-term dispersion and stability in oil base. Researchers have been more concerned about how to improve the dispersion stability of nanoparticles in water and have gained some results and experience, but these results and experience may not be suitable for oil-phase solution, because oil phase is nonpolar. In the literature on friction, wear, rheological and thermophysical characteristics, most of the authors have given very limited information about the dispersion and stabilization process of nano-lubricants/nanofluids, only giving stabilization time. As for how to extend the dispersion and stability of nanoparticles in oil base, there are even fewer reports. Therefore, how to control the coagulation of nanoparticles in oil-phase nanofluids has become the primary problem in the application of nanofluids. The nanofluid does not simply refer to a liquid–solid mixture.

As with the study of dispersion of nanoparticles in aqueous phase, some special methods and specific measures are necessary. For example, the type and concentration of surface activators or dispersants, the effect of temperature, the duration and speed of magnetic agitation, the duration and intensity of ultrasonic vibrations, and the pH value of suspensions. All these techniques aim at changing the surface properties of suspended particles and suppressing formation of particles cluster in order to obtain stable suspensions. In the same way[38], good dispersion of oil-phase nanofluids should be influenced by the factors mentioned above actually, which technique to use or to what extent depends on the case of the actual application.

To solve the compatibility problem between nanoparticles and non-aqueous solvents and to eliminate the adhesion and agglomeration problem between particles are two important factors to improve the dispersion stability. The compatibility of nanoparticles with non-aqueous solvents can be improved by adsorption of surfactants, especially polymers, onto the surface of nanoparticles. The adsorption of a surface modifier on the surface of particles act as a bridge to connect nanoparticles to the base fluids and can increase the steric resistance between particles so that the nanoparticles are dispersed in non-aqueous solvents[43]. This method has been used by many researchers to successfully disperse nanoparticles in non-aqueous solvents and keep the dispersion stable for a period of time. Some studies reported that oleic acid as a surface modifier to successfully disperse Al_2O_3 nanoparticles into lubricating oil[3, 22, 37]. When the van der Waals attraction between particles is greater than other repulsive forces,

the nanoparticles in the dispersed medium begin to condense[21]. Once large clusters or aggregates are formed, it is difficult to break them back into primary particles[44]. It can be seen from previous research results that insufficient surfactant can't form enough coating to cause electrostatic repulsion and compensate for van der Waals' attraction. However, as surfactant concentrations increase, Bridges between particle surfaces are more likely to form larger aggregates[44, 45]. Compared with other technologies, ultrasonic is undoubtedly an effective method to break up clusters and evenly distribute nanoparticles in suspension, which is also recognized by the industry. There are different technical measures for different particles to disperse into different solvents. How to use ultrasonic mode, ultrasonic frequency, ultrasonic intensity and ultrasonic duration is a subject that needs further study, because it is a complex process of chemical and physical changes, and this process is also affected by the temperature of suspension liquid, particle concentration and the concentration of Surface modifier.

The dispersion results of the previous studies show that low-frequency ultrasonic was more effective than high-frequency ultrasonic in disaggregate powder and dispersion, and 20 kHz ultrasonic probe was found to be very effective in breaking large agglomerations[44-50]. Heretofore, understanding the effect of frequency on the dispersion stability of nanoparticles in lube oils remains not discussed. So, this research point needs further study. Furthermore, several investigations have reported the effect of ultrasonic time on the dispersion properties. The results showed that the ultrasonic time required for dispersion in the polar solution was different that depend on the oil viscosity, mixing temperature and nanoparticle concentrations[51, 52].

From the above discussion, it can be concluded that various surfactants and physical processing methods were used to prepare nanolubricants based on Al_2O_3 nanoparticles. However, no long-term stability has been reported in the literature. Therefore, it is of great significance to further study and apply various technologies to prepare nanolubricants with long-term dispersion stability[53]. Hence, this paper aims to investigate the stability of Al_2O_3 nanoparticles in base oil. The dispersion performance was described by sedimentation method, TEM images, UV absorbance and DLS analysis. This paper is an effort to study the influence of the temperature, magnetic stirring time, ultrasonic amplitude and ultrasonic duration on dispersion stability of Al_2O_3 nanoparticles in base oil to preparation nanolubricants with superior dispersion stability for a long period of time.

2. Experiment

2.1 Characterization of materials

Al_2O_3 nanoparticles (NPs) were obtained from Shanghai ChaoWei nano technology Co. LTD, China. The morphology of the nanomaterials was characterized utilizing transmission electron microscopy (TEM) as displayed in Fig.1 NPs is spherical in shape and has a wide range of particle sizes, with an average particle size of about 60 nm. A synthetic base oil was chosen as the solvent to study the dispersion stability of nanoparticles, mainly because it has more practical significance than mineral oil. Poly alpha olefin (PAO6) was selected as the base oil because it is considered to be the most promising base oil for

synthetic lubricants, and it is also the most widely used for general purposes, such as engine lubricating oils, bearing oils, hydraulic oils, aviation lubricants, heat transfer fluid and grease, etc[54]. PAO6 was purchased from JingMen petrochemical company of china. Detailed specification parameters of Al₂O₃ nanoparticles and physicochemical properties of PAO6 based fluids are shown in Table 2.

Table 2
Properties of the materials:

Materials	Properties
Al ₂ O ₃ Nanoparticles	Morphology: spherical, purity: 99.99%, Average particle size: 60 nm, Color: White, Specific surface area: 58m ² /g, Apparent density of powders: 0.55g/cm ³
PAO 6	Density (°C): 0.804 g/cm ³ , Dynamic viscosity at 40 °C: 31.94 cst Dynamic viscosity at 100 °C: 5.90 cst

Figure.2 presents the XRD pattern of the Al₂O₃ nanomaterials. The diffraction of the Al₂O₃ peaks is located at $2\theta = 25.578^\circ, 35.154^\circ, 37.779^\circ, 43.357^\circ, 46.18^\circ, 52.556^\circ, 57.057^\circ$ and 68.214° which can be indexed to the (0 1 2), (1 0 4), (1 1 0), (1 1 3), (2 0 2), (0 2 4), (1 1 6) and (3 0 0), respectively. The peaks are sharp and very clear, indicating good crystallinity. These peaks were very compatible with the standard Joint Committee on Powder Diffraction Standards (JCPDS) card No. 78-2427.

Oleic acid (C₁₈H₃₄O₂) with a purity of 98.5% was used as the surfactant to keep the nanoparticles stable in the solution. The oleic acid was purchased from Sinopharm Chemical Reagent Co., Ltd.

2.2 Equipment

In this section, the main equipment and instruments used to prepare nanolubricants samples and evaluate dispersion stability are described below. Since probe sonication has the potential advantages of better particle dispersion, smaller effective diameter and higher efficiency than ultrasonication bath, we selected probe sonication for nanofluid sample preparation[55]. Transducer Digital Sonifier (Tai Wei Ultrasonic technology co. LTD, China) was used for generating the ultrasound with a maximum input power of 1200W and a frequency of 20 kHz. The output power of the generator could be regulated by adjusting the vibration amplitude. The product has a 16 mm exponential horn, piezoelectric transducers transferred the high-frequency voltage generated by the generator into mechanical vibrations and outputs it through the index horn. According to the requirements, the ultrasonic probe tip was immersed 15 mm below the solution level in each test.

Heating magnetic stirrer is another important instrument JOANLAB China. It can make the nanoparticles fully contact with the surface modifier to complete the surface modification, which plays an important role in dispersion and stability. As the ultrasonic time goes on, the sample temperature will gradually increase. Because the temperature has an important influence on the dispersion stability, in

order to avoid this negative outcome, we add a digital refrigerator bath (DC-3006-II, Shunma Inc, China) used for temperature control was connected with a recursion beaker.

2.3 Characterization of dispersion stability

Various experimental characterization techniques are applied to the qualitative and quantitative analysis of dispersion stability. Techniques such as sedimentation, particle size analysis■UV–Vis Spectroscopy and transmission electron microscopy.

2.3.1 Sedimentation

The settlement observation method is used for the qualitative analysis of dispersion stability, which is the most effective direct proof of the final result of the characterization of dispersion stability. All samples were placed in a dark room at room temperature (24°C), and a transparent/semi-transparent region and amount of sediment at the bottom of the test tube were observed by taking photos regularly every day.

2.3.2 Particle size analysis

It has to be said that measuring the effective particle size of a nanofluid by Dynamic Light Scattering (DLS) to characterize its dispersibility is a good method, and this method can timely reflect whether the nanoparticles have agglomerated and the state of agglomeration. The particle size analyzer used in this study is from the United States (NanoBrook Omni, Brookhaven Instruments Corp, USA), and its accuracy range and repeatability are 0.3 nm-10 µm and ± 1–2%, respectively. When testing and analyzing, take an appropriate amount of sample and put it in a special cuvette made of polystyrene with four sided clear to complete the test analysis, and set each sample to test 5 times to reduce the error of the result. In order to test accurately and reduce errors, for progressive time varying measurements, it is required that the nanofluid sample used for testing each time should be a sample in the middle of the container.

2.3.3 UV–Vis spectroscopy

UV–Vis spectroscopy■UV-1800PC, Meixi, China■is another effective method to evaluate the dispersion stability of nanofluids. The dispersion stability is reflected by quantitatively measuring the absorption coefficient of suspended particles in the wavelength range of 200-800nm. A high absorption coefficient means a higher mass fraction of nanoparticles suspended in solution, which means better dispersibility of the nanofluid[56]. In order to study progressive time-varying measurements, it is required that the nanofluid samples tested should be kept in a special cuvette and kept free from external pollution. Each sample is tested three times in each test.

2.3.4 Transmission electron microscopy

Transmission electron microscope (TEM) (JEM-1400Plus, JEOL, China) was used to study the morphological characteristics of the nanoparticles after ultra-sonication, and reflect the dispersion characteristics and aggregation degree of nanofluids with time. This method can directly reflect the

growth and aggregation of the nanoparticles, and whether there is any evidence of sedimentation, and it is also valid evidence for the comparison of the results. The oil adsorbed on the surface of the nanoparticles cannot be easily removed, which leads to a poor observation effect in the electron microscope, and the oil will contaminate the lens. Therefore, the oil on the surface of nanoparticles should be removed as much as possible before TEM observation. A micropipette was used to drop the sample on a porous copper grid, and then placed the copper grid on a clean filter paper with strong adsorption capacity to complete oil adsorption. The samples were placed in a drying box and kept at 240 ° C for several hours followed by subsequent analysis under TEM.

2.4 Experimental procedure

In this work, three concentrations of Al₂O₃ nanoparticles were studied, namely 0.005wt%, 0.01wt% and 0.02wt%. Both the liquid phase and solid phase were weighed with a precision balance with a resolution of 0.0001g (ME54E Switzerland). PAO6 oil and oleic acid were stirred at room temperature for 30 min, then dispersed by high-speed homogenizer for 5 min, and weighed nanoparticles were added and stirred by magnetic force for 5 h. After stirring, the solution was placed in a constant temperature water bath for dispersing with ultraphonic probe. Fig.3 shows the flowchart of the procedure to prepare samples of nanofluids.

3. Result And Discussion

3.1 Effect of mixing temperature

The influence of temperature on the dispersion stability of nanofluids was tested and analyzed. By adjusting the temperature of the circulating water bath to keep the internal temperature of the solution at a constant temperature (30 ° C, 50 ° C, 70 ° C, 90 ° C), set the ultrasonic amplitude to 60%, that is, the output power is 93 W.

During the ultrasonic process, cavitation accumulates a lot of heat, which will lead to the increase of temperature, and the increase of temperature will also lead to the decrease of liquid cavitation strength. Too high temperature will also cause the foaming of oleic acid, which will break the bond between oleic acid and Al₂O₃ NPs[57]. Therefore, in order to study the dispersion stability of Al₂O₃ in oil phase base solution, the most suitable temperature range should be determined in this discussion. Nanofluid samples were prepared and stability was analyzed.

Samples of Al₂O₃ nanofluid with 0.02wt% were prepared, Oleic acid has been used as surfactant and assumed a weight concentration of 0.5wt%.

As shown in Figure 4, nanofluids were prepared under different temperatures, and the absorbency behavior of the nanofluids was measured every day for 10 days, while pure PAO6 oil was presented as the comparison group. Besides, the samples have not shaken during all the time to really evaluate the change of natural deposition. It was found that the nanoparticles agglomerate with time and all have

different degrees of settlement. Figure.4 (b) shows the settlement after ten days. The results show that the temperature plays an important role in the stability of nanofluids. The stability of nanofluids prepared at 50 °C is better than that of other groups. This conclusion is further confirmed by UV–Vis spectroscopy absorption coefficient analysis. As shown in Figure.5, the absorption coefficient of different nanofluids decreases with the increase of time, and it can be seen that the stability of nanofluids prepared at 50 °C is the best behavior. Therefore, the temperature of the preparation process is kept at 50 °C in the subsequent scheme experiment.

3.2 Effect of surfactant concentration

In the oil-based system, Al₂O₃ nanoparticles need to be coated with surface modifiers to prepare stable nanofluids. The important role of surface modifiers in the preparation of stable oil-based nanofluids has been widely confirmed and adopted by the industry[58]. Drawing on previous research foundations and experiences, oleic acid was used as a surface modifier in this study[5, 58]. Since the alkyl chain on the other side of the oleic acid molecule is easily soluble in oil solution, the nanoparticles modified by oleic acid have lipophilicity and can be well soluble in oil. Because oleic acids contain carboxyl groups, and nano-metal oxides contain hydroxyl groups, they can undergo chemical reactions. The reaction products are linked together in the form of ionic bonds, thus forming a single molecule coating on the surface of nanoparticles, forming a microcellular shape, which can effectively avoid the contact of nanoparticles and forms a steric hindrance to prevent a large number of particles from settling. If the amount of the surfactant is too small to completely cover the surface of all particles, causing some particles to agglomerate and settle, But if the amount of the surfactant is too large, the modifier is simultaneously adsorbed on two or more adjacent Particle surfaces, bridging between particle surfaces are more likely to form larger aggregates to accelerate sedimentation and reduce the stability of the nanofluid, so matching an appropriate amount of surfactant with the nanoparticles is of great significance[41, 44, 59].

Set the mass concentration of Al₂O₃ nanofluid to 0.005wt%, 0.01wt% and 0.02wt%, and the corresponding oleic acid concentration gradients are (0.2wt%⊗0.4wt %⊗0.8wt%)⊗0.2wt%⊗0.4wt %⊗0.8wt%⊗and⊗0.2wt%⊗0.4wt%⊗0.8wt%⊗1.6wt %⊗, respectively. The nanofluid is prepared according to the preparation process in Fig. 3, and the temperature of stirring and ultrasonic process is ensured to be 50 °C. The ultrasonic amplitude is set to be 60% with 93 W mixing power, and the ultrasonic is uninterrupted for 2 hours.

As shown in Fig.6 and Fig.7, the nanofluids modified by different oleic acid concentrations have different degrees of sedimentation after ten days of placement, and too large or too small concentration is unfavorable to stability. It was found that the absorption coefficient of nanofluids reached the maximum value after 1 day of storage, which may be caused by the fact that the adsorption of the surface modifier on the nanoparticle is not a rapid response process, and it takes a certain time to complete the adsorption[60]. The nanoparticle at the bottom of the tube can be suspended again by absorbing the surface modifier. The concentration of 0.2wt% oleic acid is obviously not enough to support the modification of all nanoparticles, resulting in agglomeration and serious sedimentation of particles.

Oleic acid at a concentration of 1.6wt% can adsorb on the surface of particles in a short time to avoid agglomeration of nanoparticles and thus reduce the sedimentation. However, from Figure. 7(b), it can be seen that the absorption coefficient decreased sharply on the third day, which means that the particles grew up rapidly and aggregated, resulting in a large amount of sedimentation. This indicates that 1.6wt% oleic acid may be in excess, which makes it easier for particles to form larger aggregates. Moreover, it is difficult for particles to be broken by ultrasound, leading to rapid precipitation. It can also be seen from in Figure.7(b) that the maximum absorption coefficient of three concentrations decreased significantly in the early days after the preparation, which may be due to the insufficient ultrasonic time leading to the incomplete disaggregation of some original nanoparticles and the rapid growth of the particles. After preparation for 10 days, it can be seen from the comparison in Figure.6 (b) that the nanofluid modified by 0.8wt% oleic acid showed the least sedimentation and the best stability performance, which is also confirmed as shown in Figure.7(a) and Figure.7(b). From the above analysis, oleic acid with concentration of 0.8wt% can better modify nanoparticles with concentration of 0.02wt% NPs, played a good role of surface modifiers, and nanofluids showed good stability. According to the same test procedure and analysis method, the two Al_2O_3 samples with 0.005wt% and 0.01wt% were tested, and it can be concluded that the optimal oleic acid concentration for these two samples is 0.4wt%.

In order to confirm the modification effect of oleic acid on the nanoparticles, the "FT-IR" was used for analysis, as shown in Figure.8 The infrared absorption spectrum of oleic acid is presented in Fig.8(a) 2852cm^{-1} and 2925cm^{-1} represent the characteristic bands of $-\text{CH}_2$ and $-\text{CH}_3$ in oleic acid, respectively. The strong 1710cm^{-1} characteristic peak represents the C=O group of oleic acid. The broad peak bands at 1630cm^{-1} and 3445cm^{-1} in FT-IR of unmodified NPs (Fig.8b) are attributed to the stretching and bending bands of O-H groups on the surface of Al_2O_3 NPs, respectively. In the FT-IR spectra of Al_2O_3 modified with oleic acid (OA) in Fig.8c. Before taking FT-IR spectra, it is necessary to remove any non-adsorbed oleic acid from the surface of alumina nanoparticles. The comparison reveals the presence of oleic acid characteristic peaks (1710cm^{-1} C=O bond) in the modified Al_2O_3 spectrum. Two absorption bands at 2852cm^{-1} and 2925cm^{-1} (Fig.8c) are due to the vibrational frequencies of CH_2 and CH_3 groups of oleic acid covering the surface of nanoparticles. The above observation results of FT-IR spectra confirmed that oleic acid chemically reacted with the particle surface, and the surface of Al_2O_3 NPs was modified by oleic acid[61, 62].

3.3 Effect of ultrasonication power

In order to reduce sedimentation and achieve long-term stability, good dispersion is an essential prerequisite. Mechanical agitation is a simple physical dispersion method to break up the agglomeration of nanoparticles, which forces the aggregated particles to disaggregate by external shear stress[63]. In this study, all the experimental nanofluids were stirred by magnetic force for 5 hours before ultrasonication. Such operation can not only break the aggregated nanoparticles, but also make oleic acid fully contact and collide with nanoparticles, so that it can fully wrap on the surface of nanoparticles. Currently, ultrasonication is considered an effective method for dispersing nanoparticles[40]. Previous

ultrasonication studies have shown that continuous ultrasonication is better than pulsed ultrasonication and that there are optimal ultrasonication duration. Previous studies have shown that the optimal ultrasonication period and the ultrasonication amplitude are related to the type of base fluid, the type of nanoparticles, and the particle concentration, and is also affected by other conditions[46, 64]. In order to study the effects of ultrasonication amplitude and ultrasonication time on the dispersion stability of nanofluids, the ultrasonication output power was changed by adjusting the ultrasonication amplitude. The output power is changed by adjusting 50% amplitude, 60% amplitude, and 70% amplitude, corresponding to 77.5W, 93W, and 108.5W, respectively. Continuous ultrasonication was performed for 5h under each ultrasonication amplitude, but samples were retained at time nodes of 0.5h, 1h, 2h, 3h, 4h and 5h respectively. Therefore, 18 groups of samples were generated according to the matching combination of different ultrasonication amplitudes and ultrasonication time points, which were packed in different tubes, and the dispersion stability of 18 groups of samples with time was observed and analyzed. It should be noted that it is necessary to conduct ultrasonication for 2min for 18 groups of samples again after 6 hours of preparation and dispersion, so as to suspend the precipitated but wrapped nanoparticles in the liquid again and to prolong the stabilization time.

The influence of ultrasonication amplitude and ultrasonication duration on all nanofluid samples was characterized by UV spectrum. As shown in Figure.9, after 10 days of the preparation, the absorbance coefficients of 54 samples of three concentrations (0.005wt%, 0.01wt% and 0.02 wt.% NPs) were analyzed and characterized. It can be seen that the three concentrations of nanofluids all show large absorption coefficient values at the 70% amplitude (ultrasonication output power 108.5W), and obviously the disaggregate ability of the nanofluids at the 50% amplitude (ultrasonication output power 77.5W) is weak. It shows that the larger the amplitude in the same ultrasonic time, the better the effect of de-agglomeration, and the smaller the particles.

The absorption coefficients of 0.005wt% and 0.01wt% nanofluids increased with the increase of ultrasonication time, showing good dispersion stability. The absorption coefficient of 0.02wt% nanofluid reaches the maximum after 4 hours of ultrasonication. Increasing the ultrasonication time is not conducive to reducing the cluster size. This is because for the nanofluid with high mass concentration, the ultrasonication time is too long, and the chance of particle collision increases, thus causing particle agglomeration. Therefore, according to the above analysis, there is an optimal value of ultrasonication amplitude matching with ultrasonication duration for the preparation of long-term dispersed and stable nanofluids, that is, 0.02wt% needs 70% ultrasonication amplitude for 4 hours, 0.01wt% and 0.005wt% needs 70% ultrasonication amplitude for 5 hours.

3.4 Dispersion performance

In this section, three samples were sealed in a tube to observe the dispersion stability with time, and the dispersion stability was characterized by photo capturing, UV-Vis Spectroscopy and DLS method, reflecting the longest stability time that could be achieved.

For the three samples, the digital photos on the 20 and 160 days after ultrasonication were selected to reflect the change of the deposition of nanoparticles with time, as shown in figure.10. The photo on the 20 days after sonication showed a slight sedimentation at the bottom of the test tube, but it was not obvious. It can be found that the particle deposition of samples with a concentration of 0.02wt% is obvious after 160 days of ultrasonication, but the liquid color is still darker than that of pure PAO6 samples, indicating that the liquid contains a large number of suspended nanoparticles. Compared with the photos on the 20 days, it can be found that the amount of nanoparticle deposition of 0.005wt% and 0.01wt% NPs for the two samples has increased to a certain extent, but it is not obvious and can still maintain a good stability. It should be noted that oleic acid, as a surface modifier of nanoparticles, tends to form colloids at the bottom of the tube rather than white solid precipitates.

Figure.11 shows the relationship between the maximum absorption coefficient and storage time of the three samples. It is obvious that the higher the nanoparticle concentration, the larger the absorption coefficient. The absorption coefficients of the three samples increased rapidly with the storage time, reached a peak after 2 days, and then began to decrease to a fixed value, and the values could be kept within small range of variation for a long time. In this study, ultrasonication was repeated for 2 min at the 6 hours after the preparation, so that the particles which had settled to the bottom of the test tube but had been coated with oleic acid floated up again, so the absorption coefficient of the second day test reached the maximum. It can be found that the absorption coefficient of 0.02wt% nanofluid decreases significantly after 134 days, while 0.01wt% and 0.005wt% can maintain the stability for 160 days, and the stability trend of 0.005wt is better, which is also consistent with the settlement situation in the photo in Fig.10.

In the process of preparing nanofluids, the main concern is to obtain uniform suspension of nanoparticles by reducing the particle size of agglomerated nanoparticles. Particle size test can also reflect the effect of ultrasonication cracking on agglomeration and the effect of surface modifiers, so it is necessary to characterize and analyze the particle size at different time after preparation. Based on the previous analysis, the particle size of the three samples was analyzed, and the results are shown in Figure.12.

It can be found that the effective minimum particle size of the three samples are basically the same, showing a bimodal distribution. The existence of large particles indicates that a small part of clusters had not been broken completely. It also shows that under the same ultrasonication condition, the particle size obtained has little relationship with the concentration of nanofluids. For both 0.01wt% and 0.02wt% samples, the large particle size distribution disappeared after the 10 days, because the previous large particle size nanoclusters continued to grow over time until it was difficult to overcome gravity and lead to sedimentation. Due to the steric effect of oleic acid on the surface modification of nanoparticles, the growth and agglomeration trend of clusters are weak, which can make the particle size change little in a long period of time. After the tenth day of preparation, the particle sizes of the three samples gradually increased with time, but the increase was not significant. For 134 days after preparation, the particle size of the 0.02wt% nanofluid increased greatly, and the proportion of the large particle size was large,

indicating that the particles grew significantly and clusters occurred, resulting in sedimentation. For 160 days after preparation, the particle size of 0.01wt% and 0.005wt% nanofluids also increased. However, the apparent deposition phenomenon is not obvious, and it still shows good stability.

Compared with the above methods, TEM is considered as one of the important tools to determine the particle size distribution and morphology of nanoparticles. TEM micrographs were taken for the three concentrations for the samples after directly mixing and 160 days after preparation. Since the oil cannot be evaporated to a sufficient extent, it can be seen from the TEM microphotograph that all the nanoparticles are distributed within the range of the oil blot. It can be seen from the photos at the initial stage after preparation in Fig. 13 that not all the original clusters have been completely de-agglomerated, except for the large clusters, the distribution of other particle sizes has little difference, which also verifies the particle size distribution in Fig. 12. From the TEM microphotograph on the 160 days after preparation, it can be seen that the 0.02wt% nanofluid has undergone severe agglomeration, which will inevitably lead to the deposition, the decrease of absorption coefficient, and cannot maintain stability for a long time. However, although 0.005wt% nanofluid and 0.01wt% nanofluid also show a certain tendency of agglomeration, the clusters with large particle size are less and can still remain stable. The situation reflected in the TEM microphotograph is consistent with the sedimentation of the nanofluid observed in the test tube photograph, which also accords with the tendency of the absorption coefficient to change with time.

4. Conclusion

The research work is to improve the dispersion stability of Al_2O_3 nanoparticles with in base oil (PA06) and to study the influence of temperature, nanoparticles concentration, ultrasonication amplitude and ultrasonication duration on the dispersion behavior. For the three concentrations of nanofluids, the influence law of different factors was obtained, the matching combination of ultrasonication amplitude and ultrasonication duration was obtained, and the preparation process of nanofluids was innovatively optimized. The results showed that Al_2O_3 nanoparticles dispersed in the oil base at a temperature range of about 50°C was favorable, the concentration of 0.005wt% and 0.01wt% nanoparticles must be 0.4wt% oleic acid, and 0.02wt% nanoparticles must be 0.8wt% oleic acid to meet the surface modification of nanoparticles. Due to the large oil viscosity, both large-amplitude ultrasonication and long-duration ultrasonication are conducive to particle de-agglomeration, but there is an optimal matching between the ultrasonic amplitude and the ultrasonic time for different particle concentration. The results showed that the nanofluids with concentrations of 0.005wt% and 0.01wt% could be stable with low sedimentation for more than 160 days at 70% ultrasound amplitude for 5 h, while 0.02wt% could be stable with low sedimentation for up to 134 days at 70% ultrasonication amplitude for 4 h, Which is probably the longest period of stability reported so far. The results also show that the smallest attainable size after ultrasonication is not closely related to the particle concentration.

Declarations

Acknowledgments

The authors would like to express their deep appreciation to the support by the National Natural Science Foundation of China (NSFC, Project No. 51875423) and Innovative Research Team Development Program of Ministry of Education of China (IRT_17R83) and 111 Project-B17034 for the research work. The authors also would like to acknowledge the support by the Hubei Key Laboratory of Advanced Technology for Automotive Components (Wuhan University of Technology). We also express our sincere appreciation to those anonymous reviewers and editors for their meaningful and favorable advice.

Declaration of interests

The authors declare that they have no known competing financial interests or personal relationships that could have appeared to influence the work reported in this paper.

CRediT author statement

Haijun Liu: Writing - Original Draft, Data Curation, Validation, Writing–Review & Editing.

Xianjun Hou: Conceptualization, Methodology, Project administration,

Xiaoxue Li: Data Curation, Resources. Funding acquisition.

Mohamed. Kamal. Ahmed. Ali: Formal analysis, Supervision.

Hua Jiang: Investigation.

Zekun Tian: Resources.

References

1. M.K.A. Ali, P. Fuming, H.A. Younus, M.A.A. Abdelkareem, F.A. Essae, A. Elagouz, H. Xianjun, Fuel economy in gasoline engines using $\text{Al}_2\text{O}_3/\text{TiO}_2$ nanomaterials as nanolubricant additives, *Applied Energy*, 211 (2018) 461-478.
2. Z.S. Zhao, Y.S. Zhang, S.F. Wang, K. Guo, J. Tang, Z.G. Wu, G. Zhang, Y.X. Zhu, P.X. Yan, W.Y. Zhang, Tribological properties of oleylamine-modified nickel nanoparticles as lubricating oil additive, *Materials Research Express*, 6 (2019) 105037.
3. M.K.A. Ali, H. Xianjun, M. Liqiang, C. Qingping, R.F. Turkson, C. Bicheng, Improving the tribological characteristics of piston ring assembly in automotive engines using Al_2O_3 and TiO_2 nanomaterials as nano-lubricant additives, *Tribology International*, 103 (2016) 540-554.
4. M.K.A. Ali, H. Xianjun, F.A. Essa, M.A.A. Abdelkareem, A. Elagouz, S.W. Sharshir, Friction and wear reduction mechanisms of the reciprocating contact interfaces using nanolubricant under different loads and speeds, *Journal of Tribology*, 140 (2018).

5. M.K.A. Ali, H. Xianjun, A. Elagouz, F.A. Essa, M.A.A. Abdelkareem, Minimizing of the boundary friction coefficient in automotive engines using Al_2O_3 and TiO_2 nanoparticles, *J Nanopart Res*, 18 (2016) 377.
6. S.J. Asadauskas, R. Kreivaitis, G. Bikulčius, A. Grigucevičienė, J. Padgurskas, Tribological effects of Cu, Fe and Zn nano-particles, suspended in mineral and bio-based oils, *Lubrication Science*, 28 (2016) 157–176.
7. M. Asnida, S. Hisham, N.W. Awang, A.K. Amirruddin, M.M. Noor, K. Kadirkama, D. Ramasamy, G. Najafi, F. Tarlochan, Copper (II) oxide nanoparticles as additive in engine oil to increase the durability of piston-liner contact, *Fuel*, 212 (2018) 656-667.
8. M.H. Esfe, M.R. Sarlak, Experimental investigation of switchable behavior of CuO-MWCNT (85%–15%)/10W-40 hybrid nano-lubricants for applications in internal combustion engines, *Journal of Molecular Liquids*, 242 (2017) 326-335.
9. M.H. Esfe, A.A.A. Arani, S. Esfandeh, M. Afrand, Proposing new hybrid nano-engine oil for lubrication of internal combustion engines: Preventing cold start engine damages and saving energy, *Energy*, 170 (2019) 228-238.
10. A.H.a. Battez, J.L. R. González , J.E. Viesca, J.M. Fernández , D.I. Fernández, A. Machadoc, J.R. R. Choud, CuO, ZrO_2 and ZnO nanoparticles as antiwear additive in oil lubricants, *Wear*, 265 (2008) 422–428.
11. S. Ingole, A. Charanpahari, A. Kakade, S.S. Umare, D.V.B. c, J. Menghani, Tribological behavior of nano TiO_2 as an additive in base oil, *Wear*, 301 (2013) 776-785.
12. D. Jiao, S. Zheng, Y. Wang, R. Guan, B. Cao, The tribology properties of alumina/silica composite nanoparticles as lubricant additives, *Applied Surface Science*, 257 (2011) 5720-5725.
13. P.-P. Laura, T.-T. Jaime, G. Lorena, M.-C. Demófilo, M. Remigiusz, L. Carolina, Effect of CuO and Al_2O_3 nanoparticle additives on the tribological behavior of fully formulated oils, *Wear*, 332 (2015) 1256-1261.
14. X.F. Sun, Y.L. Qiao, W. Song, S.N. Ma, C.H. Hu, High Temperature Tribological Properties of Modified Nanodiamond Additive in Lubricating Oil, *Physics Procedia*, 50 (2013) 343-347.
15. J. Padgurskas, R. Rukuiza, I. Prosyčovas, R. Kreivaitis, Tribological properties of lubricant additives of Fe, Cu and Co nanoparticles, *Tribology International*, 60 (2013) 224-232.
16. Z. Chen, X. Liu, Y. Liu, Ultrathin MoS_2 nanosheets with superior extreme pressure property as boundary lubricants, *SCIENTIFIC REPORTS*, 5 (2015).
17. W. Zhai, W. Lu, X. Liu, L. Zhou, Nanodiamond as an effective additive in oil to dramatically reduce friction and wear for fretting steel/copper interfaces, *Tribology International*, 129 (2019) 75-81.
18. V. Zin, F. Agresti, S. Barison, The synthesis and effect of copper nanoparticles on the tribological properties of lubricant oils, *IEEE TRANSACTIONS ON NANOTECHNOLOGY*, 12 (2013) 751-759.
19. L. Joly-Pottuz, B. Vacher, N. Ohmae, Anti-wear and friction reducing mechanisms of carbon nano-onions as lubricant additives, *TRIBOLOGY LETTERS*, 30 (2008) 69-80.

20. Q. Zhou, J. Huang, J. Wang, Z. Yang, S. Liu, Z. Wang, S. Yang, Preparation of a reduced graphene oxide/zirconia nanocomposite and its application as a novel lubricant oil additive, *RSC Advances*, 5 (2015) 91802-91812.
21. M.K.A. Ali, H. Xianjun, R.F. Turkson, Z. Peng, C. Xiandong, Enhancing the thermophysical properties and tribological behaviour of engine oils using nano-lubricant additives, *RSC Advances*, 6 (2016) 77913-77924.
22. R. Xu, X. Yu, Q. Zou, Effect of particle concentration on tribological properties of ZnO nanofluids, *Tribology Transactions*, 60 (2016) 154-158.
23. X.H. Kang, B. Wang, L. Zhu, H. Zhu, Synthesis and tribological property study of oleic acid-modified copper sulfide nanoparticles, *Wear*, 265 (2008) 150-154.
24. H.-I. Yu, Y. Xu, S. Pei-jing, Tribological properties and lubricating mechanisms of Cu nanoparticles in lubricant, *TRANSACTIONS OF NONFERROUS METALS SOCIETY OF CHINA*, 18 (2008) 636-641.
25. Z.Y. Lu, Z.Z. Cao, E.Z. Hu, Preparation and tribological properties of WS₂ and WS₂/TiO₂ nanoparticles, *Tribology International*, 130 (2019) 308-316.
26. J.-W. An, D.-H. You, D.-S. Lim, Tribological properties of hot-pressed alumina–CNT composites, *Wear*, 255 (2003) 677-681.
27. A. Elagouz, M.K.A. Ali, X.J. Hou, M.A.A. Abdelkareem, M.A. Hassan, Frictional performance evaluation of sliding surfaces lubricated by zinc-oxide nano-additives, *Surface Engineering*, (2019) 1-14.
28. J.M. Liñeira del Río, E.R. López, J. Fernández, F. García, Tribological properties of dispersions based on reduced graphene oxide sheets and trimethylolpropane trioleate or PAO 40 oils, *Journal of Molecular Liquids*, 274 (2019) 568-576.
29. A. Sajeeb, P.K. Rajendrakumar, Investigation on the rheological behavior of coconut oil based hybrid CeO₂/CuO nanolubricants, *Journal of Engineering Tribology*, 233 (2018) 170-177.
30. N. Rajendhran, S. Palanisamy, P. Periyasamy, R. Venkatachalam, Enhancing of the tribological characteristics of the lubricant oils using Ni-promoted MoS₂ nanosheets as nano-additives, *Tribology International*, 118 (2018) 314-328.
31. Y. Meng, F.H. Su, Y.Z. Chen, Au/Graphene oxide nanocomposite synthesized in supercritical CO₂ fluid as energy efficient lubricant additive, *ACS Appl Mater Interfaces*, 9 (2017) 39549-39559.
32. C.P. Koshy, P.K. Rajendrakumar, M.V. Thottackkad, Evaluation of the tribological and thermo-physical properties of coconut oil added with MoS₂ nanoparticles at elevated temperatures, *Wear*, 330 (2015) 288-308.
33. N. Mohan, M. Sharma, R. Singh, N. Kumar, Tribological properties of automotive Lubricant SAE 20W-40 Containing nano-Al₂O₃ particles, *SAE Technical Paper Series*, 2014.
34. V. Zin, F. Agresti, S. Barison, Tribological properties of engine oil with carbon nano-horns as nano-additives, 55 (2014) 45-53.
35. T. Luo, X.W. Wei, H.Y. Zhao, G.Y. Cai, X.Y. Zheng, Tribology properties of Al₂O₃/TiO₂ nanocomposites as lubricant additives, *Ceramics International*, 40 (2014) 10103-10109.

36. W. Li, S.H. Zheng, B.Q. Cao, S.Y. Ma, Friction and wear properties of ZrO_2/SiO_2 composite nanoparticles, *Journal of Nanoparticle Research*, 13 (2010) 2129-2137.
37. M. Kole, T.K. Dey, Enhanced thermophysical properties of copper nanoparticles dispersed in gear oil, *Applied Thermal Engineering*, 56 (2013) 45-53.
38. M. Kole, T.K. Dey, Effect of aggregation on the viscosity of copper oxide-gear oil nanofluids, *International Journal of Thermal Sciences*, 50 (2011) 1741-1747.
39. N.W. Awang, D. Ramasamy, K. Kadirkama, M. Samykano, G. Najafi, N.A.C. Sidik, An experimental study on characterization and properties of nano lubricant containing Cellulose Nanocrystal (CNC), *International Journal of Heat and Mass Transfer*, 130 (2019) 1163-1169.
40. M.K.A. Ali, H. Xianjun, Improving the heat transfer capability and thermal stability of vehicle engine oils using Al_2O_3/TiO_2 nanomaterials, *Powder Technology*, 363 (2020) 48-58.
41. B. LotfizadehDehkordi, S.N. Kazi, M. Hamdi, A. Ghadimi, E. Sadeghinezhad, M. H. S. C., Investigation of viscosity and thermal conductivity of alumina nanofluids with addition of SDBS, *Heat Mass Transfer*, 49 (2013) 1109–1115.
42. H.E. Mohammad, A. Ali, Esfandeh, Saeed, Proposing new hybrid nano-engine oil for lubrication of internal combustion engines: Preventing cold start engine damages and saving energy, *Energy*, 170 (2019) 228-238.
43. V.S. Nguyen, D. Rouxel, B. Vincent, Dispersion of nanoparticles: from organic solvents to polymer solutions, *Ultrason Sonochem*, 21 (2014) 149-153.
44. V.S. Nguyen, D. Rouxel, R. Hadji, B. Vincent, Y. Fort, Effect of ultrasonication and dispersion stability on the cluster size of alumina nanoscale particles in aqueous solutions, *Ultrason Sonochem*, 18 (2011) 382-388.
45. A. Ghadimi, R. Saidur, H.S.C. Metselaar, A review of nanofluid stability properties and characterization in stationary conditions, *International Journal of Heat and Mass Transfer*, 54 (2011) 4051-4068.
46. I.M. Mahbubul, R. Saidur, M.A. Amalina, E.B. Elcioglu, T. Okutucu-Ozyurt, Effective ultrasonication process for better colloidal dispersion of nanofluid, *Ultrason Sonochem*, 26 (2015) 361-369.
47. K. Anand, V. Siby, Role of surfactants on the stability of nano-zinc oxide dispersions, *Particulate Science and Technology*, 35 (2015) 67-70.
48. Y.L. Zhai, L. Li, J. Wang, Z.H. Li, Evaluation of surfactant on stability and thermal performance of Al_2O_3 -ethylene glycol (EG) nanofluids, *Powder Technology*, 343 (2019) 215-224.
49. J.E. Graves, M. Sugden, R.E. Litchfield, D.A. Hutt, T.J. Mason, A.J. Cobley, Ultrasound assisted dispersal of a copper nanopowder for electroless copper activation, *Ultrason Sonochem*, 29 (2016) 428-438.
50. J.X. Guo, G.C. Barber, D.J. Schall, Q. Zou, S.B. Jacob, Tribological properties of ZnO and WS_2 nanofluids using different surfactants, *Wear*, 382-383 (2017) 8-14.
51. I.M. Mahbubul, E.B. Elcioglu, R. Saidur, M.A. Amalina, Optimization of ultrasonication period for better dispersion and stability of TiO_2 -water nanofluid, *Ultrason Sonochem*, 37 (2017) 360-367.

52. M.K.A. Ali, H. Xianjun, M.A.A. Abdelkareem, Anti-wear properties evaluation of frictional sliding interfaces in automobile engines lubricated by copper/graphene nanolubricants, *Friction* 2019. <https://doi.org/10.1007/s40544-019-0308-0>
53. N. Sezer, M.A. Atieh, M. Koç, A comprehensive review on synthesis, stability, thermophysical properties, and characterization of nanofluids, *Powder Technology*, 344 (2019) 404-431.
54. R. Chou, A.H. Battez, J.J. Cabello, J.L. Viesca, A. Osorio, A. Sagastume, Tribological behavior of polyalphaolefin with the addition of nickel nanoparticles, *Tribology International*, 43 (2010) 2327-2332.
55. F.R. Siddiqui, C.Y. Tso, K.C. Chan, S.C. Fu, C.Y.H. Chao, On trade-off for dispersion stability and thermal transport of Cu-Al₂O₃ hybrid nanofluid for various mixing ratios, *International Journal of Heat and Mass Transfer*, 132 (2019) 1200-1216.
56. A. Ghadimi, I.H. Metselaar, The influence of surfactant and ultrasonic processing on improvement of stability, thermal conductivity and viscosity of titania nanofluid, *Experimental Thermal and Fluid Science*, 51 (2013) 1-9.
57. V. Raman, A. Abbas, Experimental investigations on ultrasound mediated particle breakage, *Ultrason Sonochem*, 15 (2008) 55-64.
58. C. Choi, H.S. Yoo, J.M. Oh, Preparation and heat transfer properties of nanoparticle-in-transformer oil dispersions as advanced energy-efficient coolants, *Current Applied Physics*, 8 (2008) 710-712.
59. M. Abdullah, S.R. Malik, M.H. Iqbal, M.M. Sajid, N.A. Shad, S.Z. Hussain, W. Razzaq, Y. Javed, Sedimentation and stabilization of nano-fluids with dispersant, *Colloids and Surfaces A: Physicochemical and Engineering Aspects*, 554 (2018) 86-92.
60. L. Yang, K. Du, X.F. Niu, Y.J. Li, Y. Zhang, An experimental and theoretical study of the influence of surfactant on the preparation and stability of ammonia-water nanofluids, *International Journal of Refrigeration*, 34 (2011) 1741-1748.
61. E. Soleimani, N. Zamani, Surface Modification of Alumina Nanoparticles: A dispersion study in organic media, *Acta Chim Slov*, 64 (2017) 644-653.
62. A.R. Mahdavian, Y. Sarrafi, M. Shabankareh, Nanocomposite particles with core–shell morphology III: preparation and characterization of nano Al₂O₃–poly(styrene–methyl methacrylate) particles via miniemulsion polymerization, *Polymer Bulletin*, 63 (2009) 329-340.
63. X.L. Song, S.T. Huang, B.Y. Gong, R.B. Meng, M.W. Zhang, Y.Z. Yang, Y.S. Zhong, N. Jiang, Synthesis of γ-Al₂O₃/CeO₂ coated nanoparticles and dispersion stability of their suspension, *Integrated Ferroelectrics*, 146 (2013) 76-87.
64. M.E. Kabir, M.C. Saha, S. Jeelani, Effect of ultrasound sonication in carbon nanofibers/polyurethane foam composite, *Materials Science and Engineering: A*, 459 (2007) 111-116.

Figures

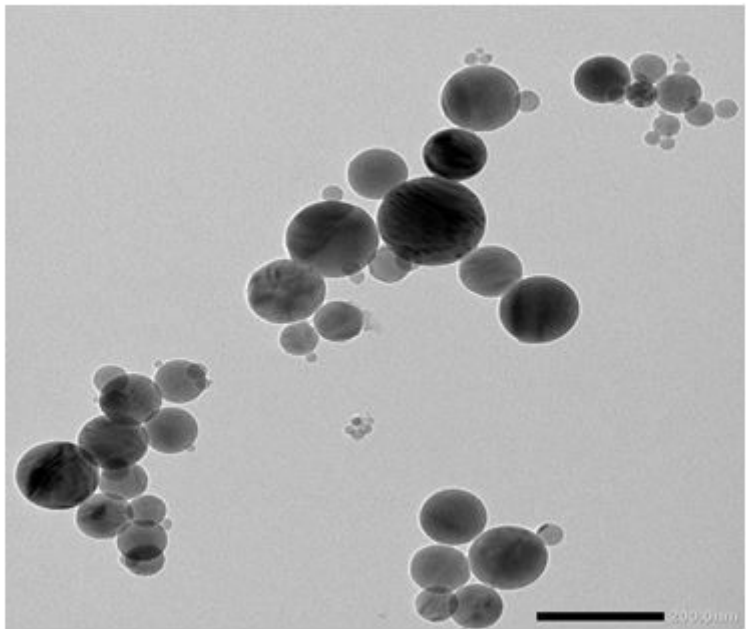


Figure 1

TEM image of Al₂O₃ nanoparticles with an average diameter of 60 nm

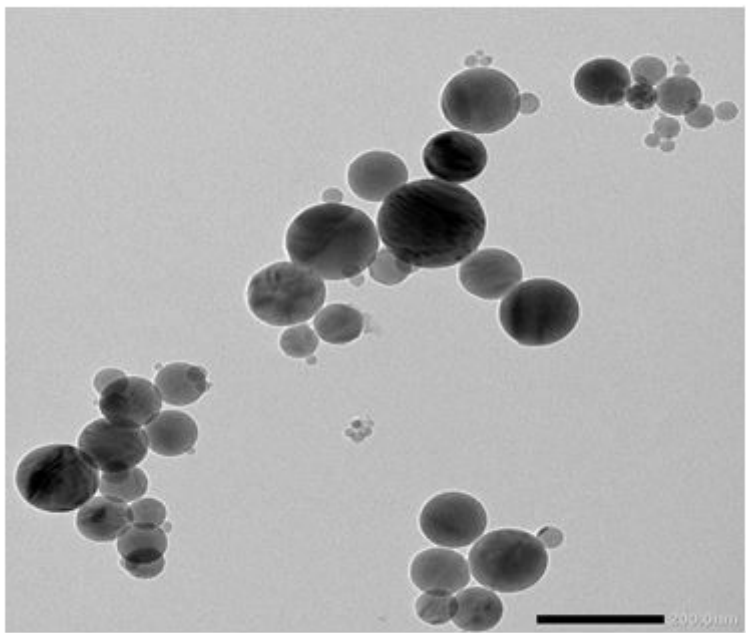


Figure 1

TEM image of Al₂O₃ nanoparticles with an average diameter of 60 nm

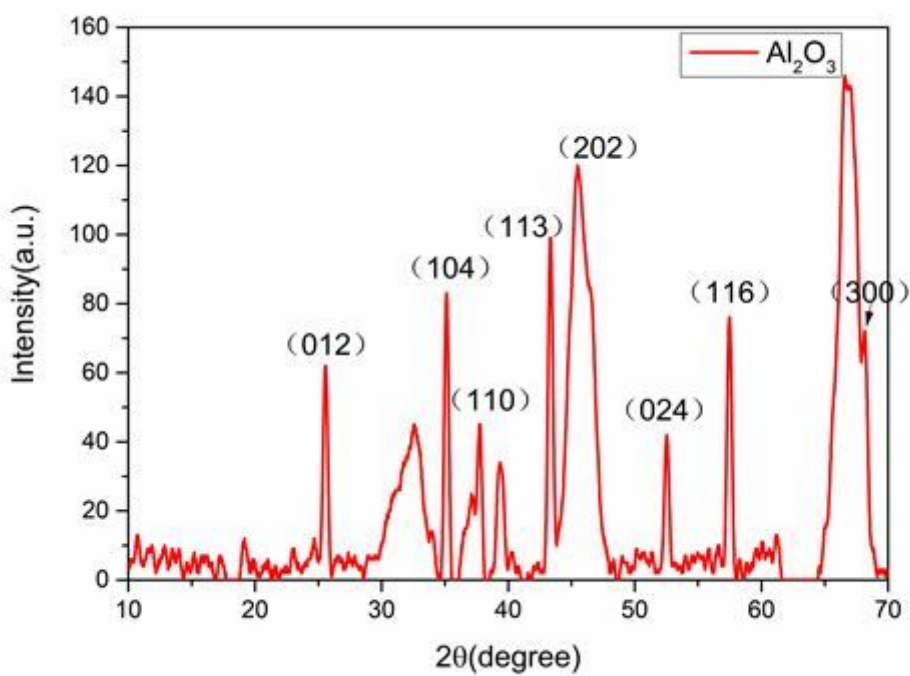


Figure 2

XRD patterns of Al₂O₃ nanoparticles.

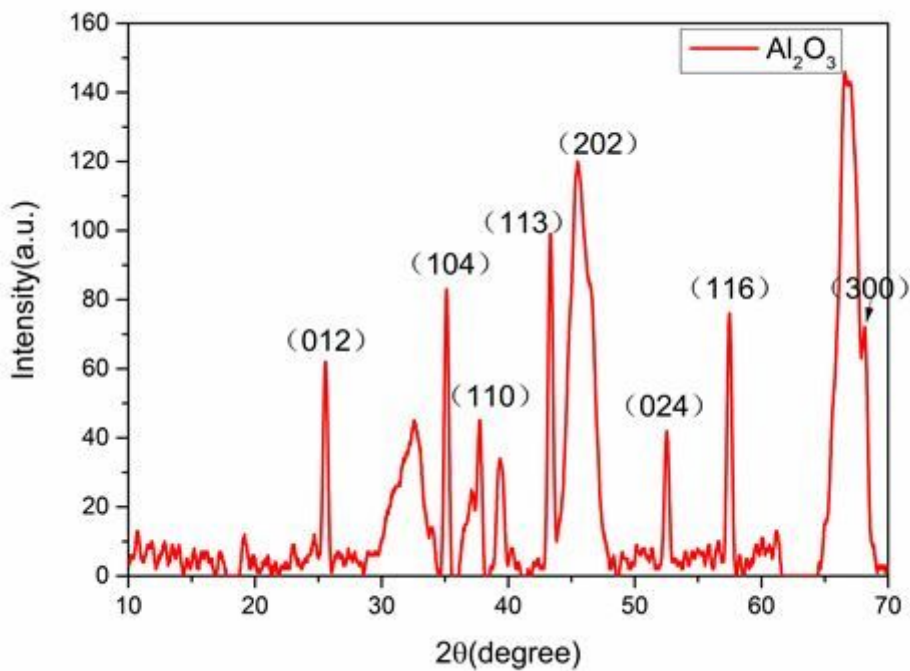


Figure 2

XRD patterns of Al₂O₃ nanoparticles.

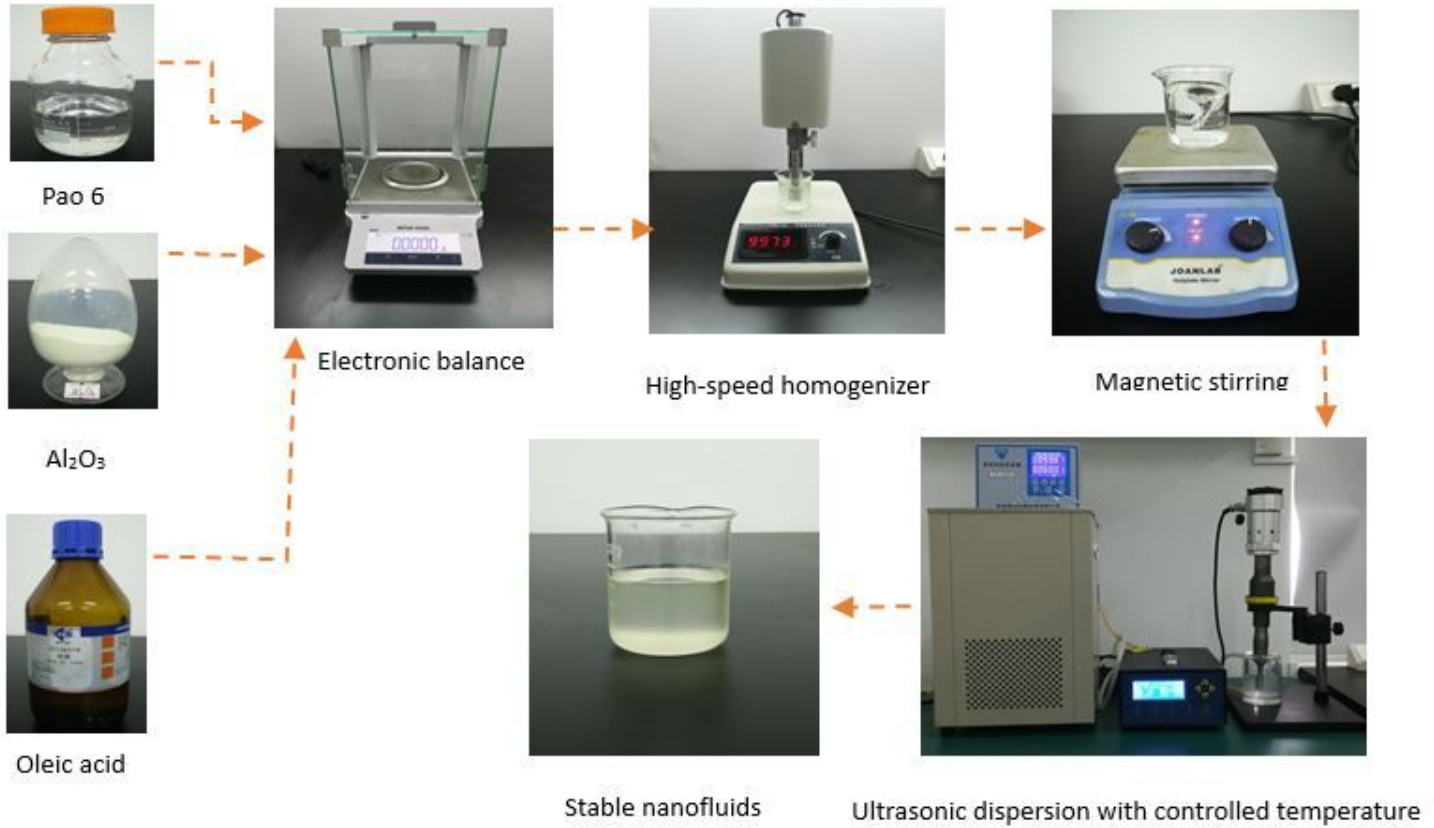


Figure 3

The flowchart of the procedure to prepare samples of nanofluids

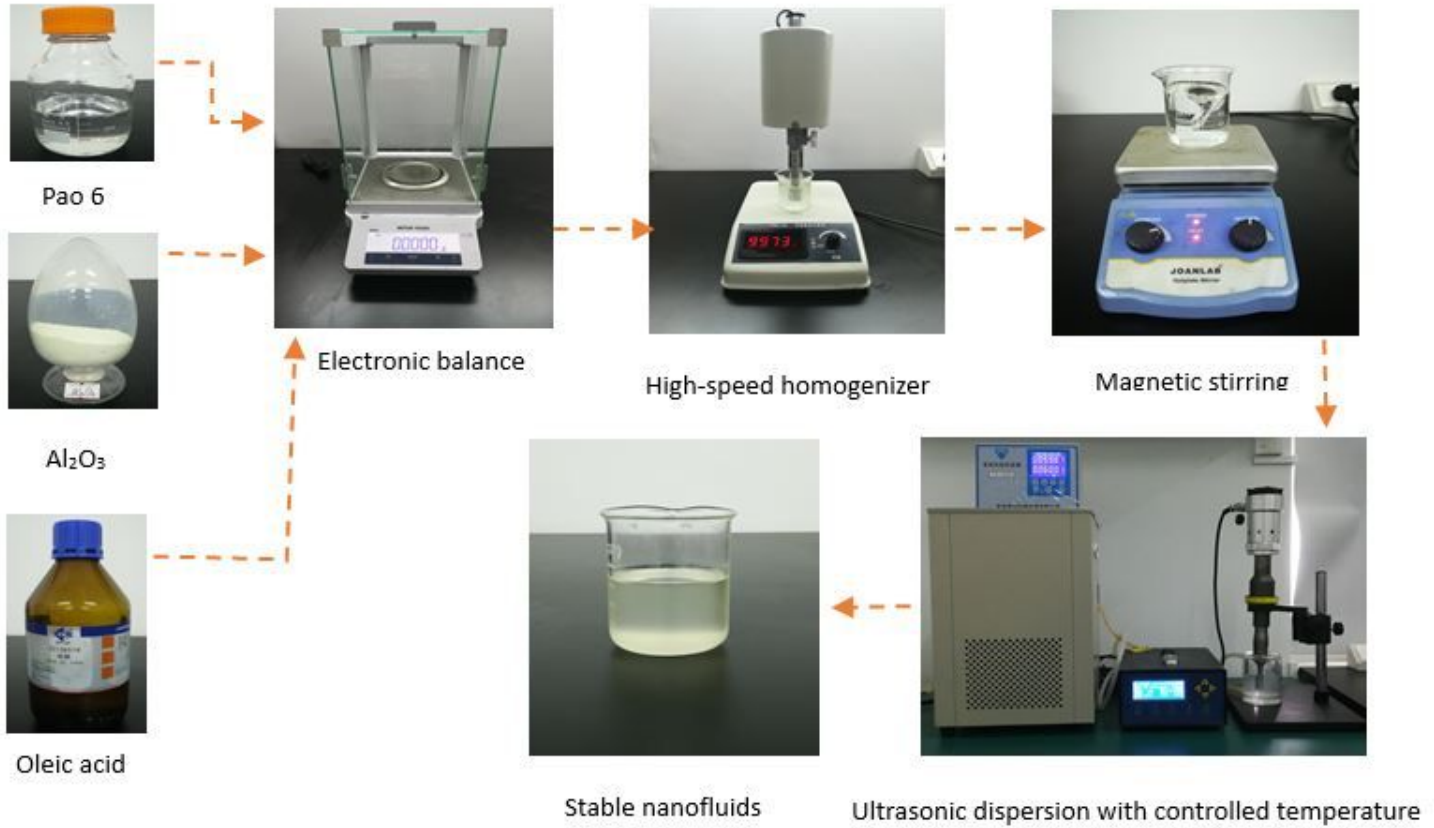


Figure 3

The flowchart of the procedure to prepare samples of nanofluids

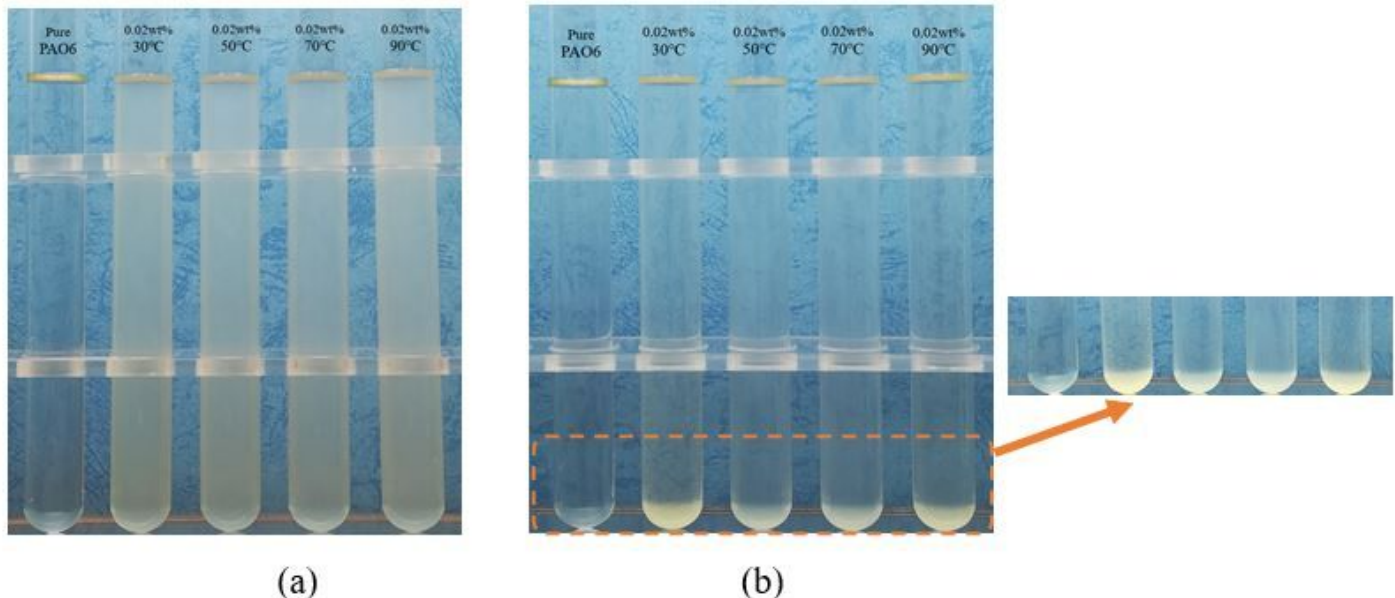


Figure 4

Photo capturing of the effect of temperature on Al₂O₃ nanofluid at just prepared and 10 days after preparation; (a) After preparation and (b) After 10 days.

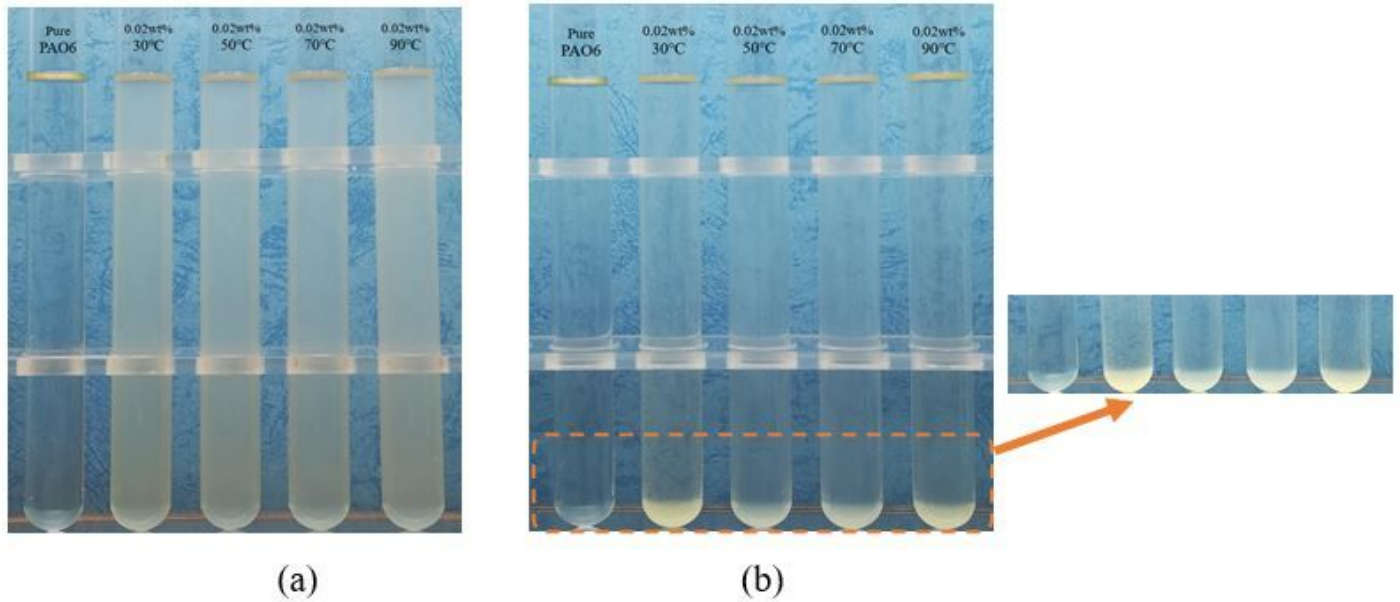
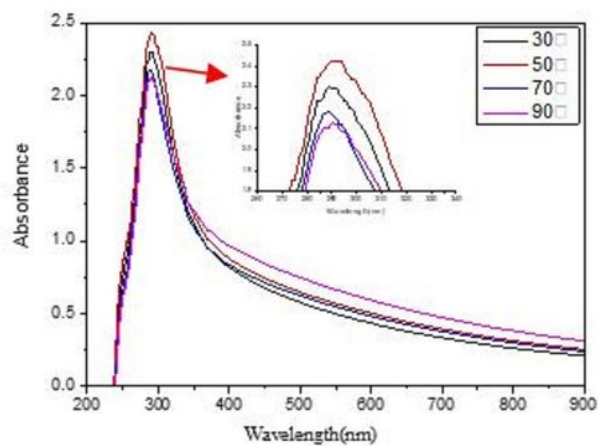
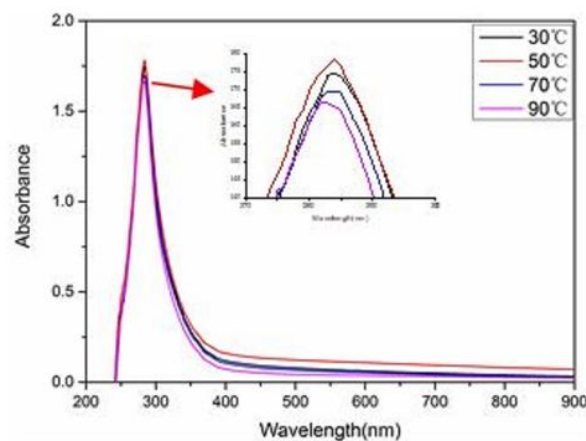


Figure 4

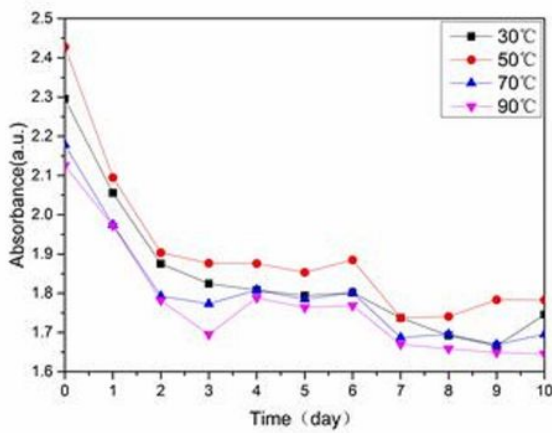
Photo capturing of the effect of temperature on Al₂O₃ nanofluid at just prepared and 10 days after preparation; (a) After preparation and (b) After 10 days.



(a)



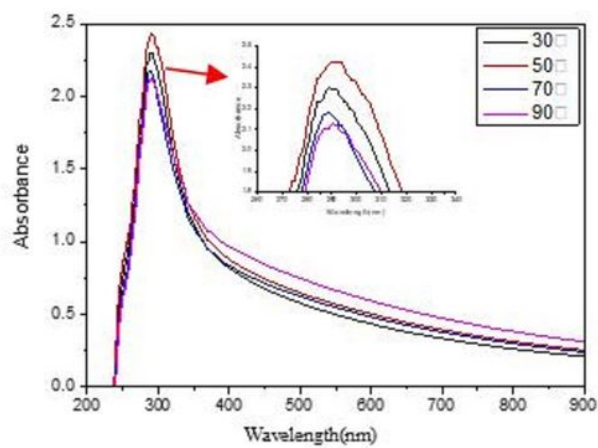
(b)



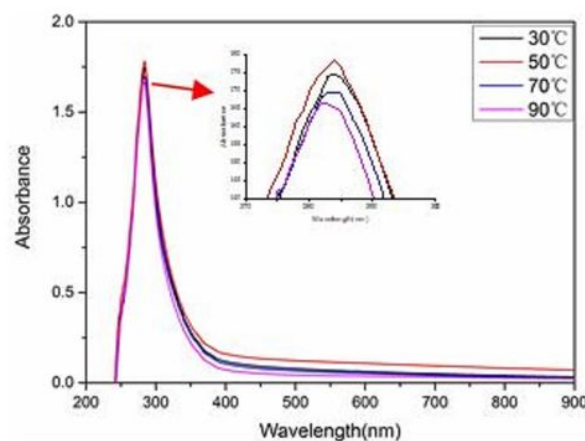
(c)

Figure 5

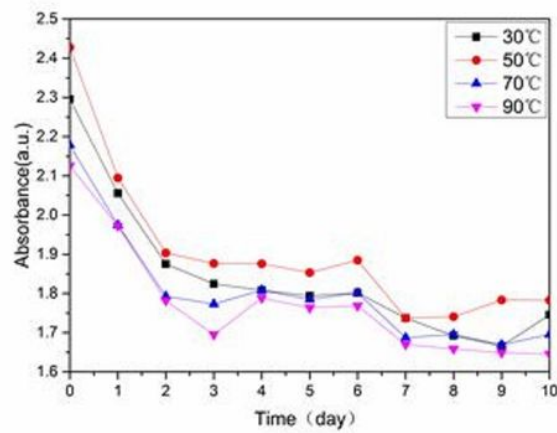
The absorbency behavior of nanolubricants with time (a) After preparation and(b) After 10 days and(c) Change of absorption coefficient with time



(a)



(b)



(c)

Figure 5

The absorbency behavior of nanolubricants with time (a) After preparation and(b) After 10 days and(c) Change of absorption coefficient with time

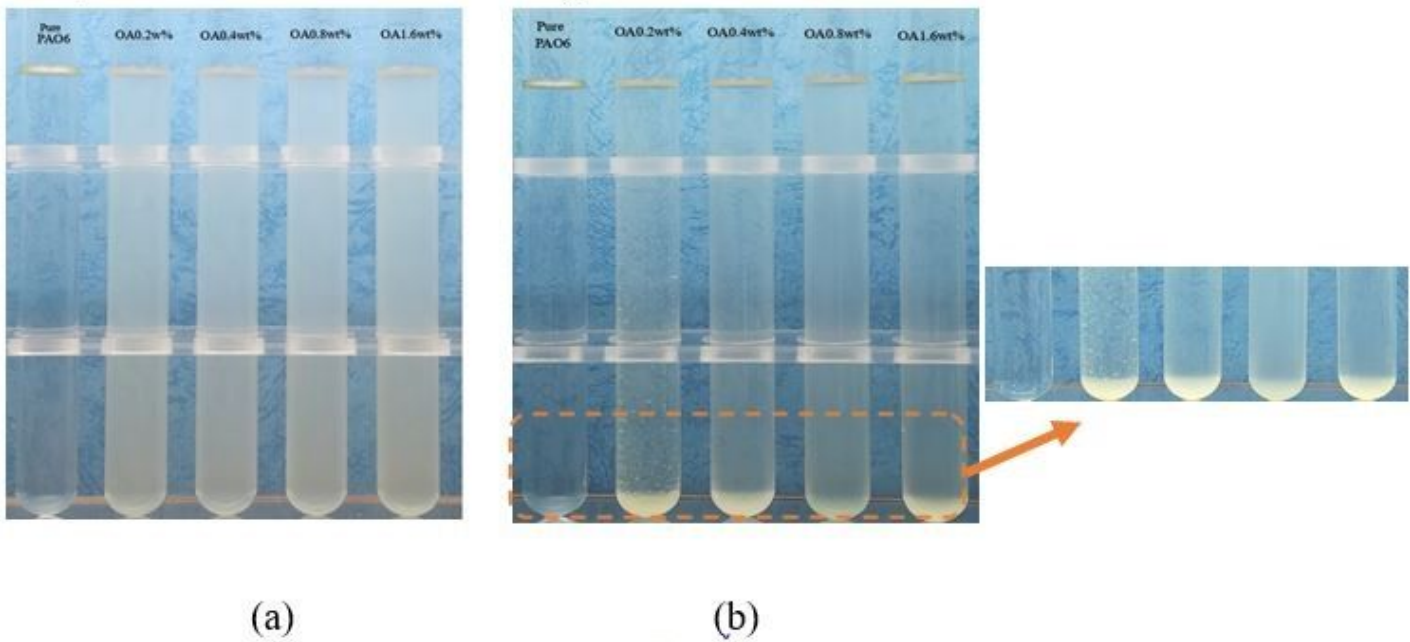


Figure 6

Photo capturing of the effect of acid concentration on Al₂O₃ nanofluid at just prepared and 10 days after preparation; (a) After preparation and(b) After 10 days

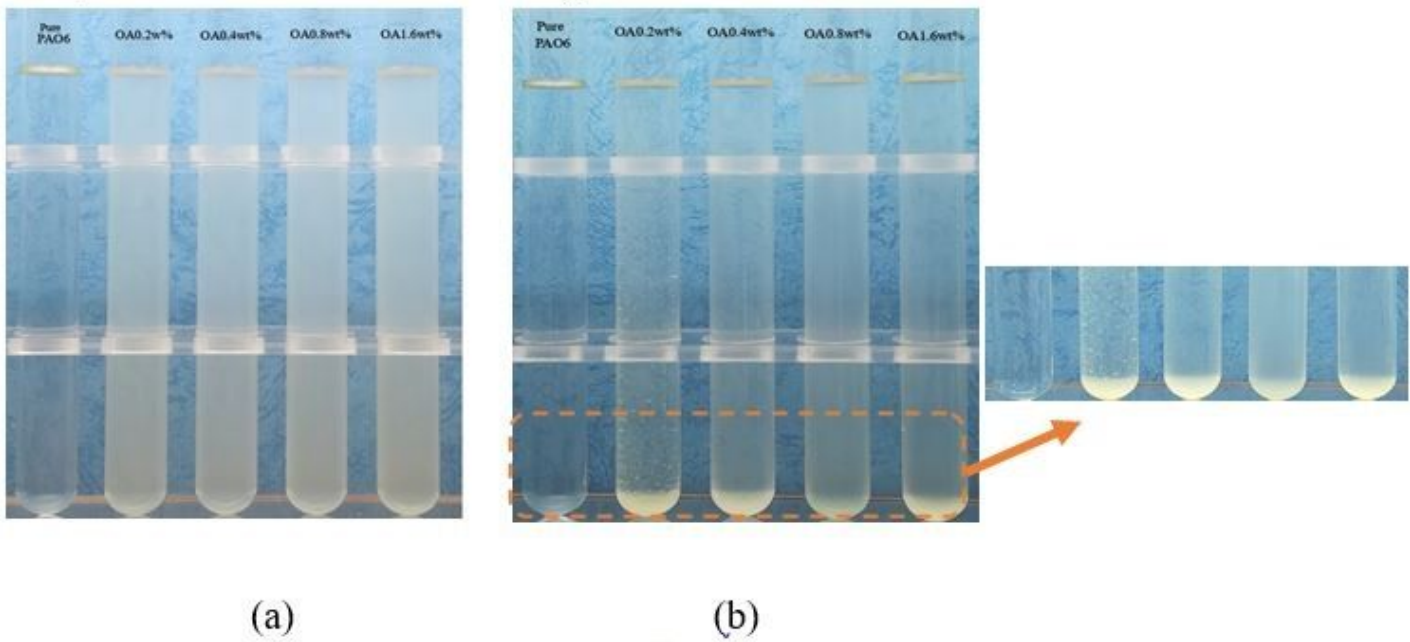
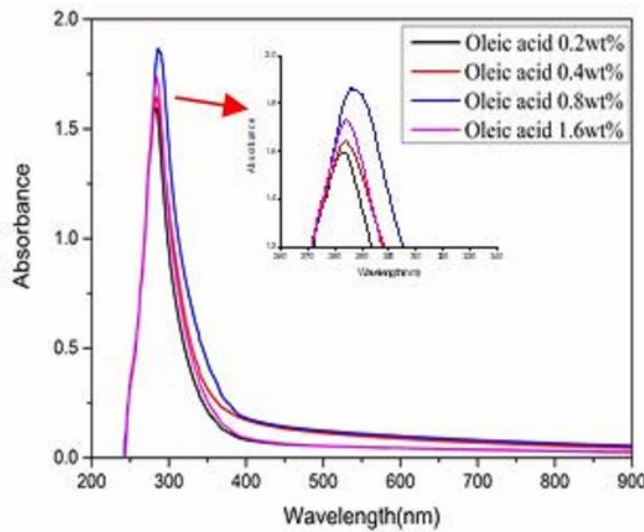
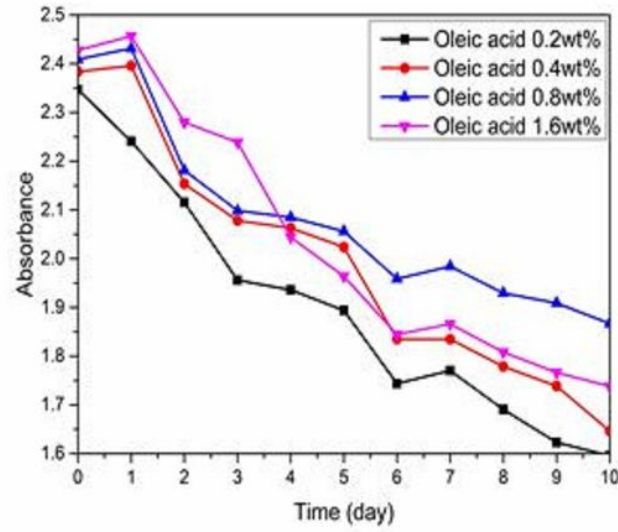


Figure 6

Photo capturing of the effect of acid concentration on Al₂O₃ nanofluid at just prepared and 10 days after preparation; (a) After preparation and(b) After 10 days



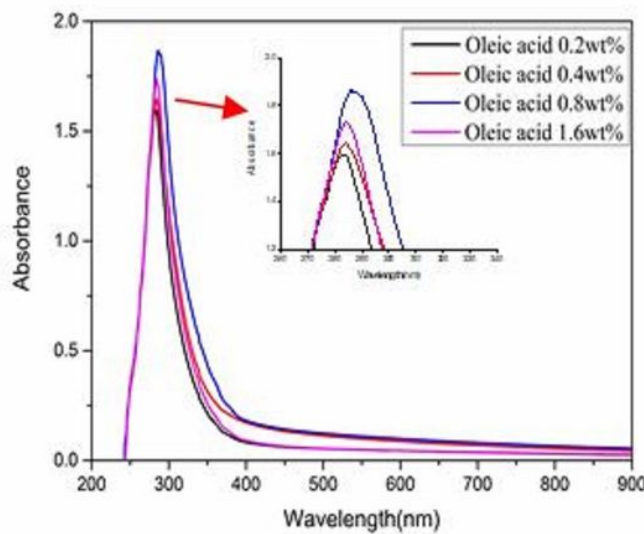
(a)



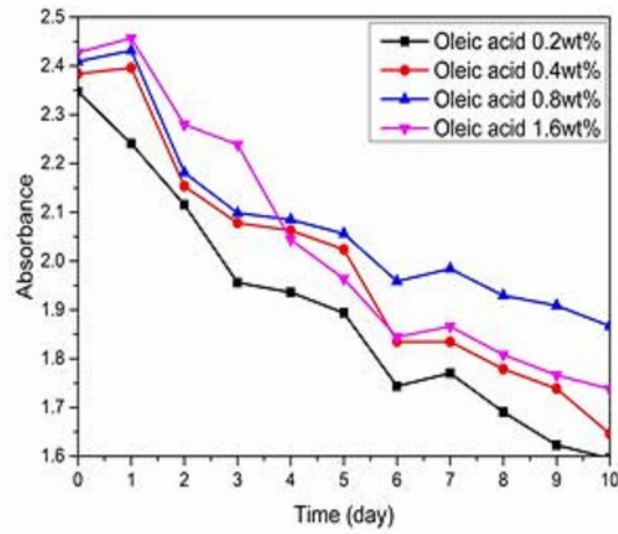
(b)

Figure 7

Absorption spectra of dispersions of Al₂O₃ nanofluids with time (a) After 10 days and(b) Change of absorbance within 10 days



(a)



(b)

Figure 7

Absorption spectra of dispersions of Al₂O₃ nanofluids with time (a) After 10 days and(b) Change of absorbance within 10 days

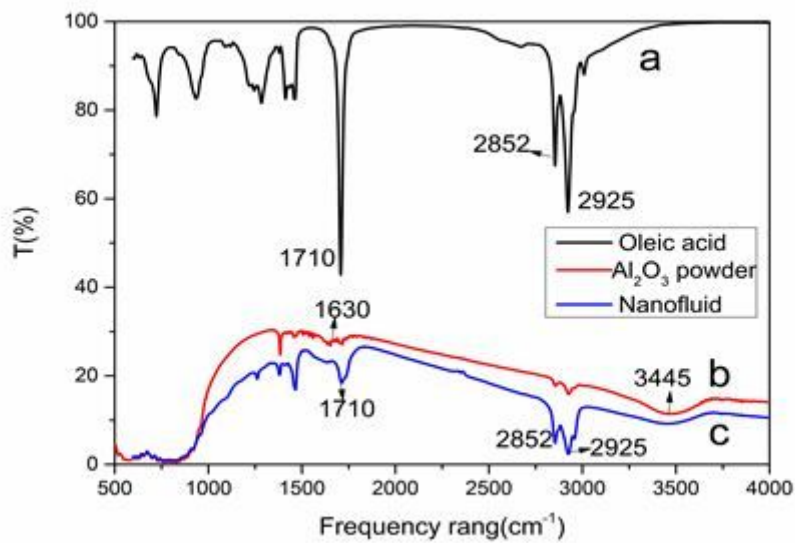


Figure 8

FT-IR spectra of: (a) oleic acid (b) bare Al₂O₃ NPs; (c) Al₂O₃ NPs modified by oleic acid

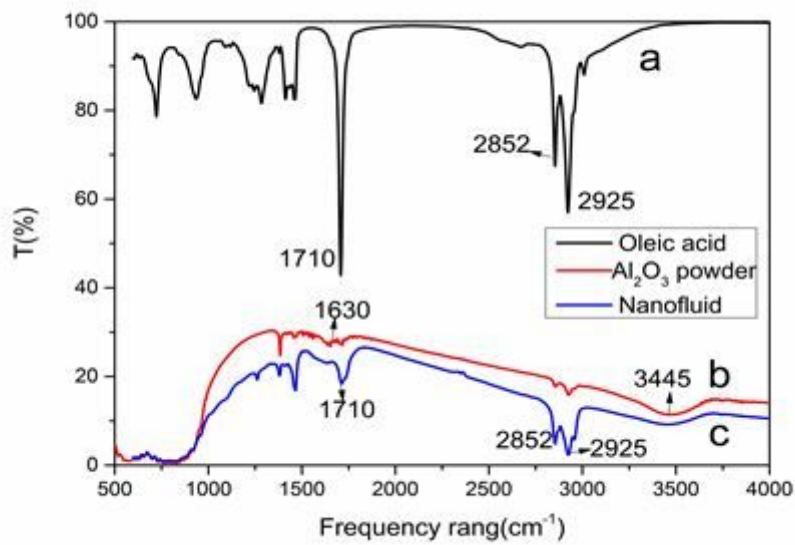


Figure 8

FT-IR spectra of: (a) oleic acid (b) bare Al₂O₃ NPs; (c) Al₂O₃ NPs modified by oleic acid

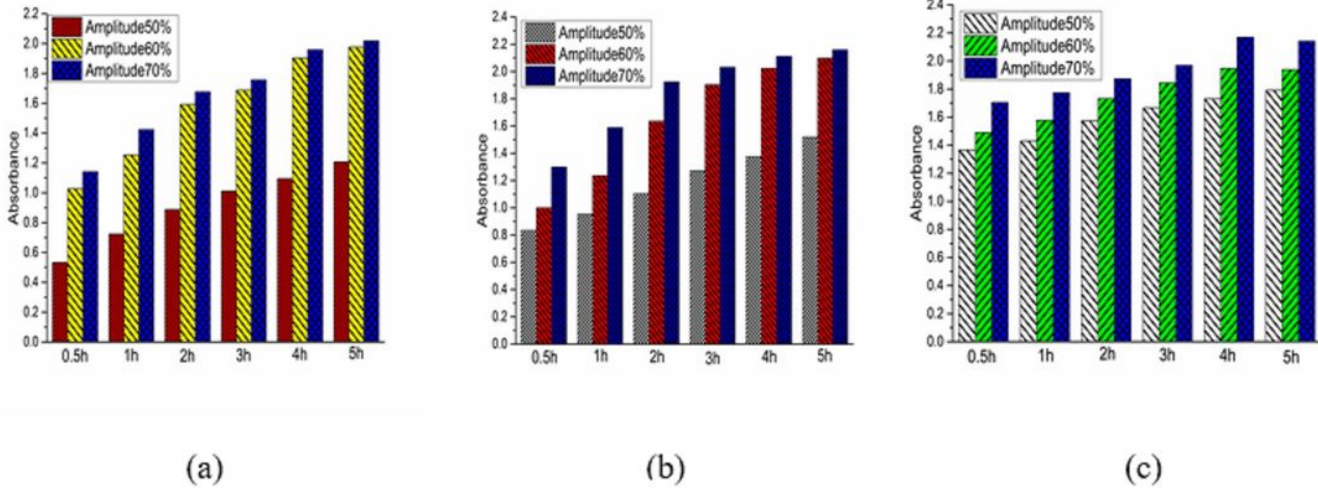


Figure 9

Maximum absorption coefficient of Al₂O₃ nanolubricants for 10days after preparation using 20 kHz, 50%, 60%, and 70% amplitude ultrasonication under mixing time of 0-5 hours: (a) For 0.005wt% NPs and(b) For 0.01wt% NPs and(c) For 0.02wt% NPs

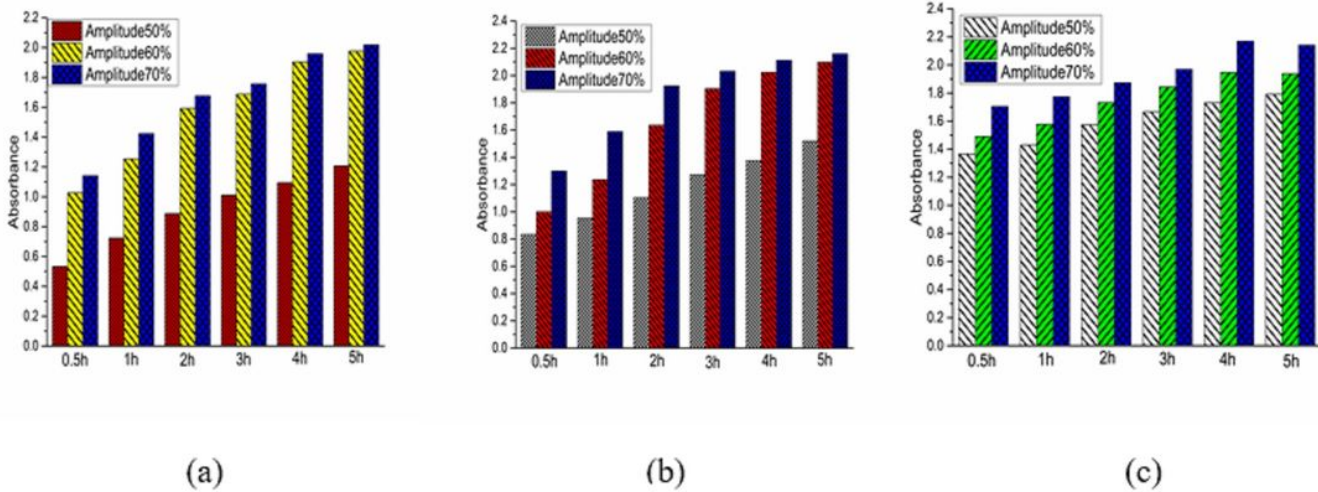


Figure 9

Maximum absorption coefficient of Al₂O₃ nanolubricants for 10days after preparation using 20 kHz, 50%, 60%, and 70% amplitude ultrasonication under mixing time of 0-5 hours: (a) For 0.005wt% NPs and(b) For 0.01wt% NPs and(c) For 0.02wt% NPs

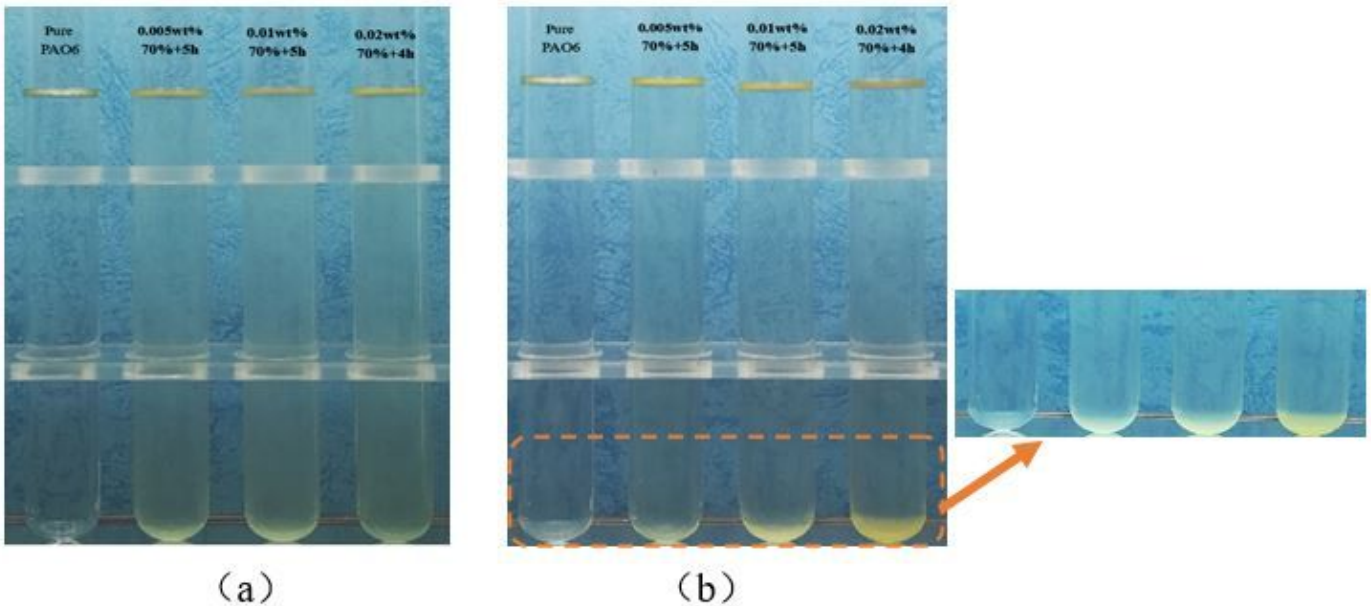


Figure 10

Photo capturing of Al₂O₃ nanoparticles dispersed in PAO6, 20 kHz, 70% amplitude (a) On the 20th day after preparation and (b) On the 160th day after preparation

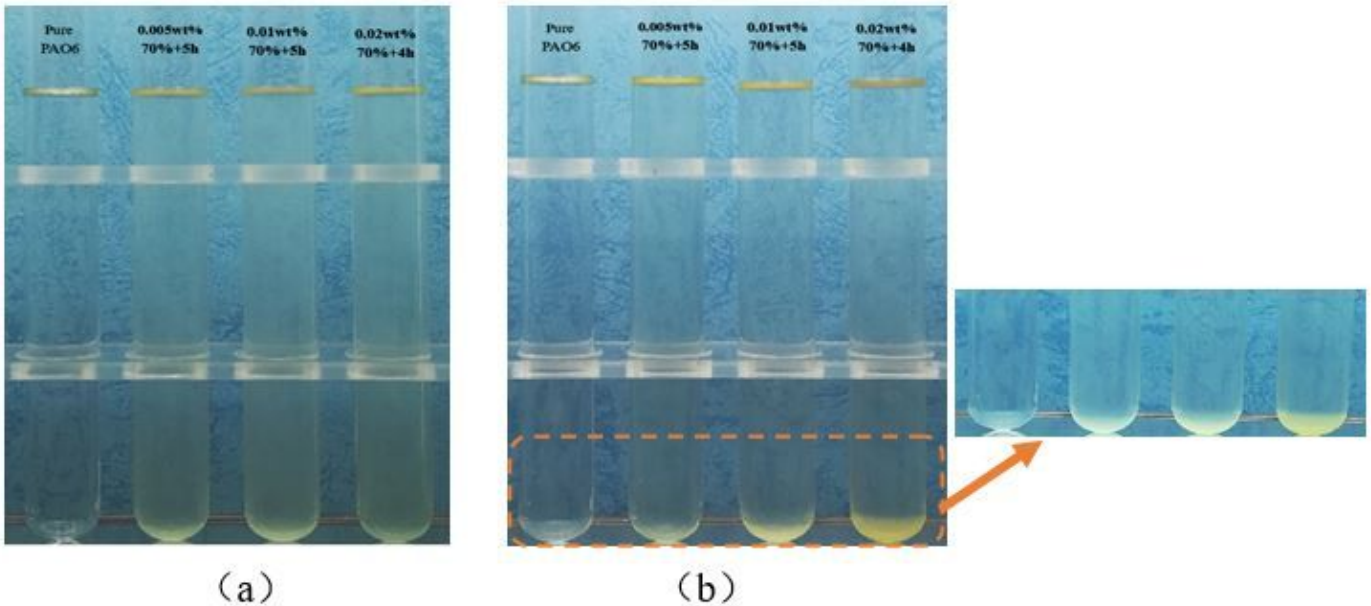


Figure 10

Photo capturing of Al₂O₃ nanoparticles dispersed in PAO6, 20 kHz, 70% amplitude (a) On the 20th day after preparation and (b) On the 160th day after preparation

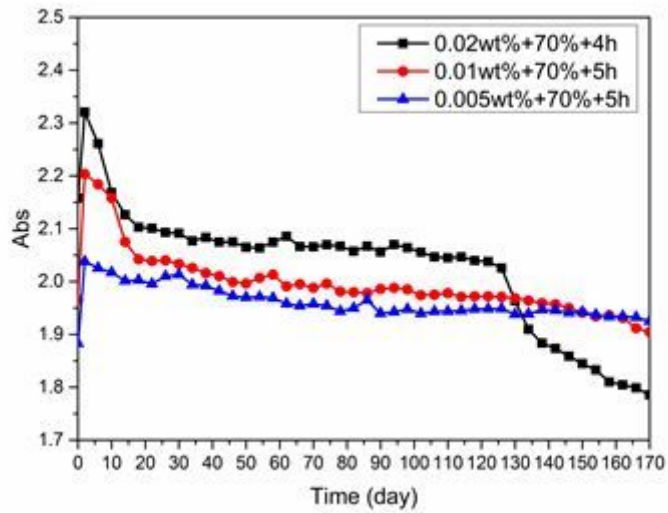


Figure 11

The relation of absorption coefficient of Al₂O₃ nanoparticles with time

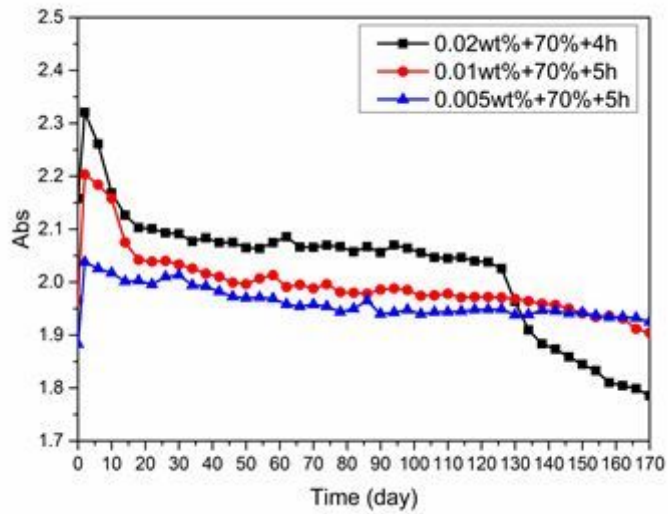


Figure 11

The relation of absorption coefficient of Al₂O₃ nanoparticles with time

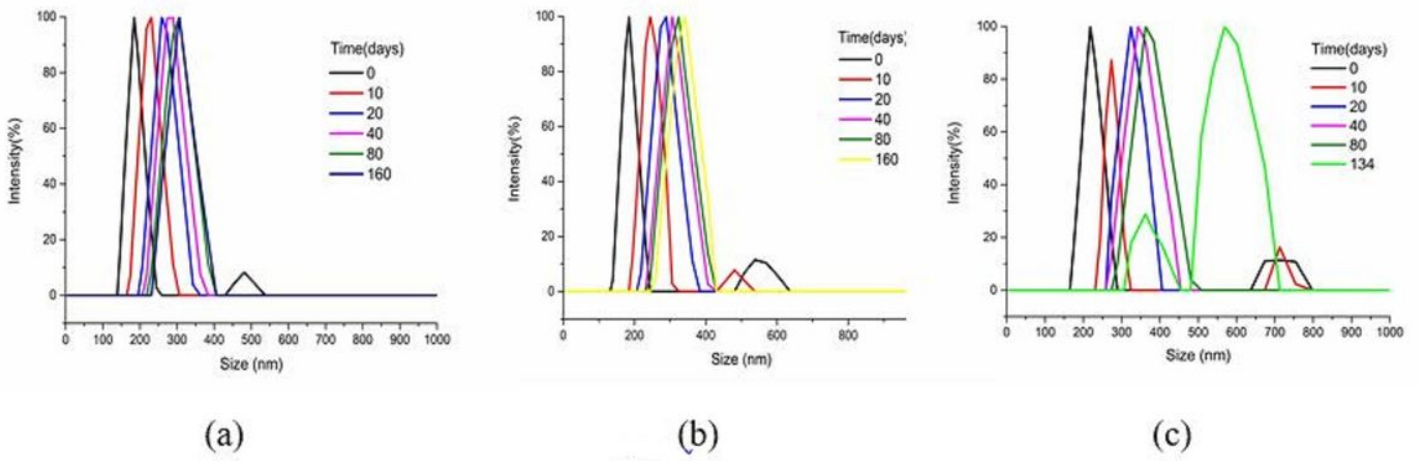


Figure 12

the particle size of Al₂O₃ nanoparticles changes with time (a) 0.005wt% NPs and (b) 0.01wt% NPs and (c) 0.02wt% NPs.

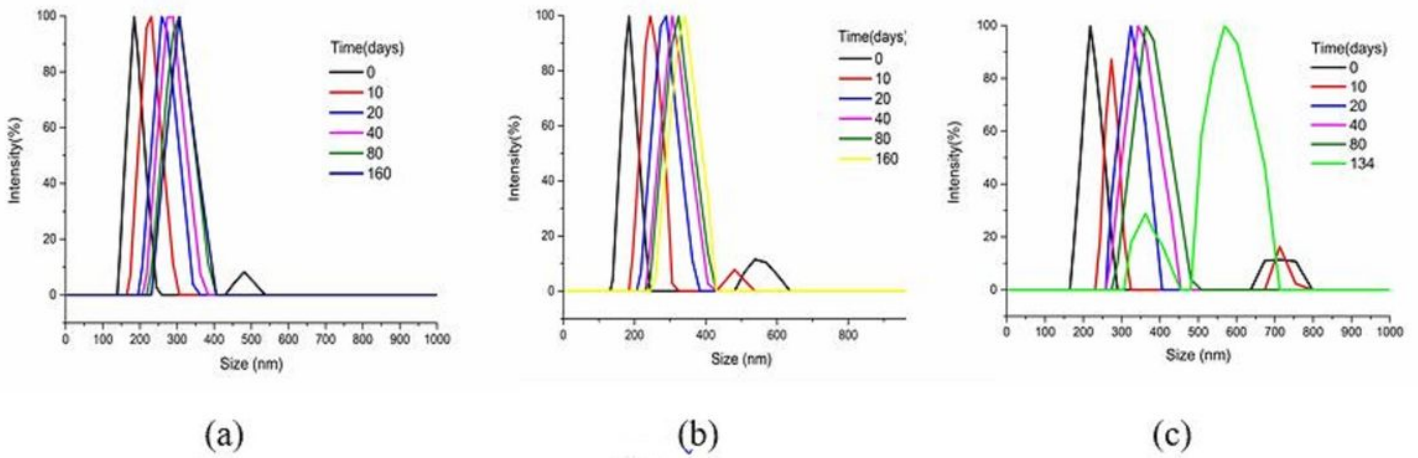
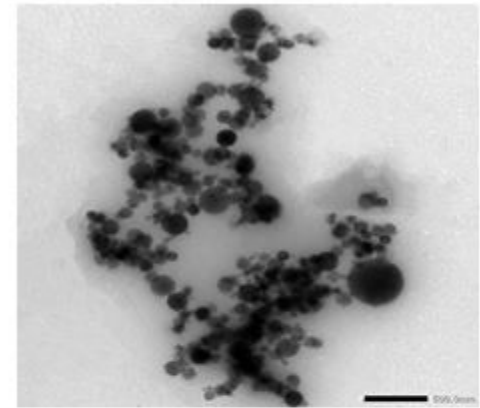
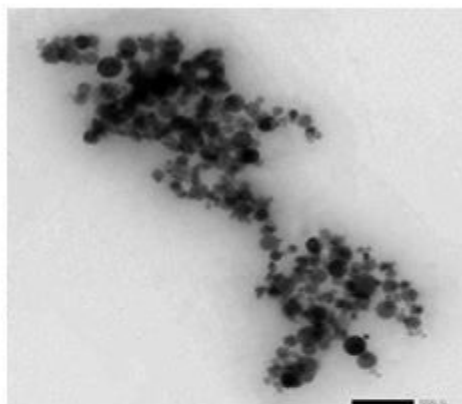


Figure 12

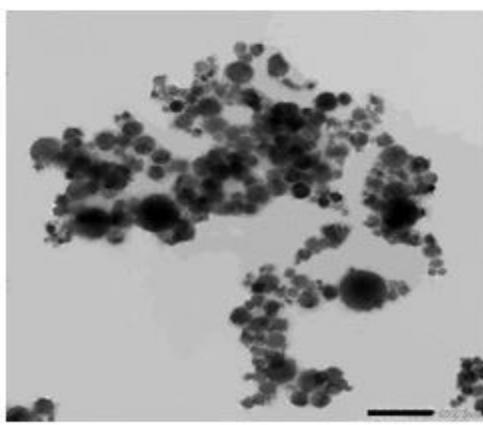
the particle size of Al₂O₃ nanoparticles changes with time (a) 0.005wt% NPs and (b) 0.01wt% NPs and (c) 0.02wt% NPs.



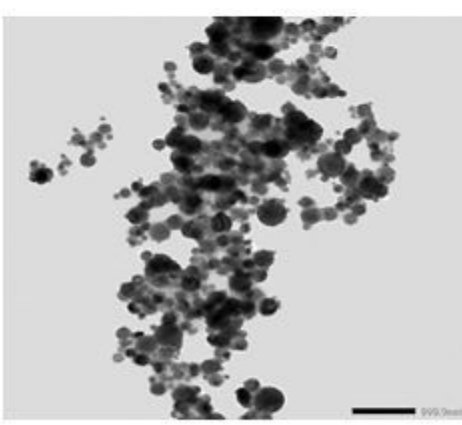
(a)



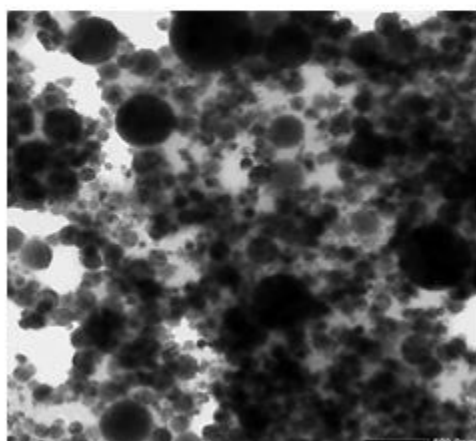
(b)



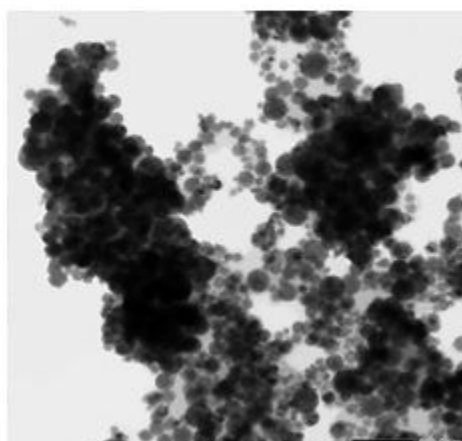
(c)



(d)



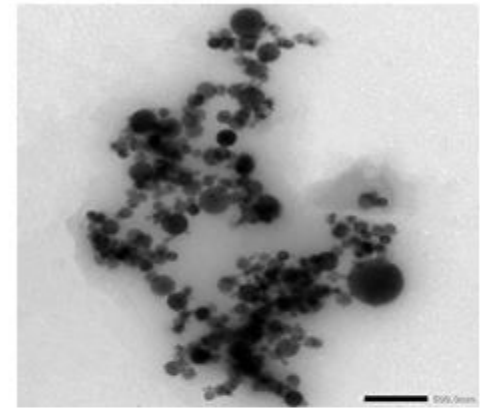
(e)



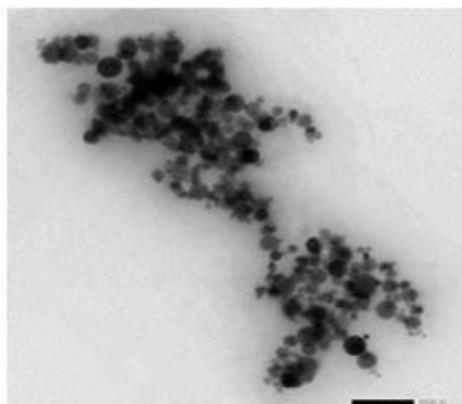
(f)

Figure 13

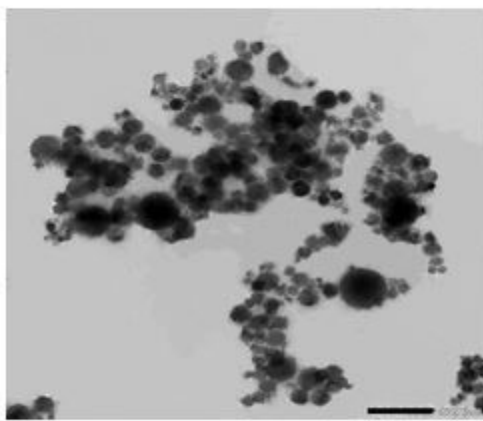
TEM micrographs of Al₂O₃ nanoparticles dispersed in PAO6 under 20 kHz, 70% amplitude. (a-c-e) For 0.005wt%, 0.01wt% and 0.02wt% NPs after preparation and (b-d-f) For 0.005wt%, 0.01wt% and 0.02wt% NPs after 160 days.



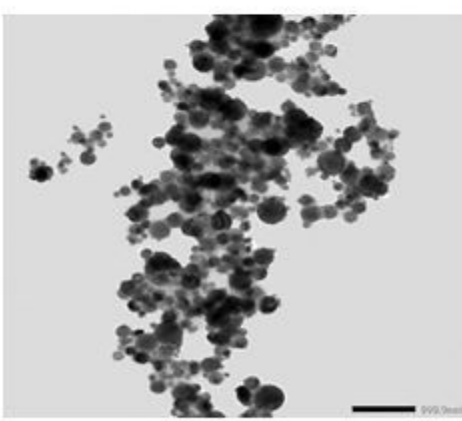
(a)



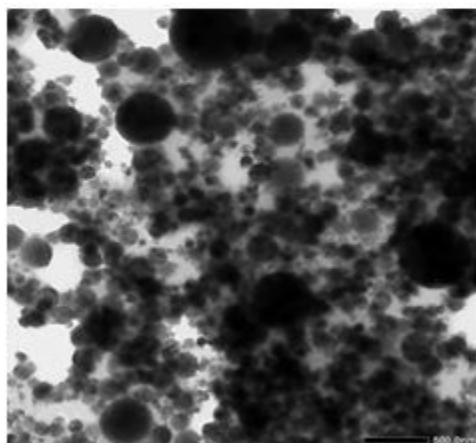
(b)



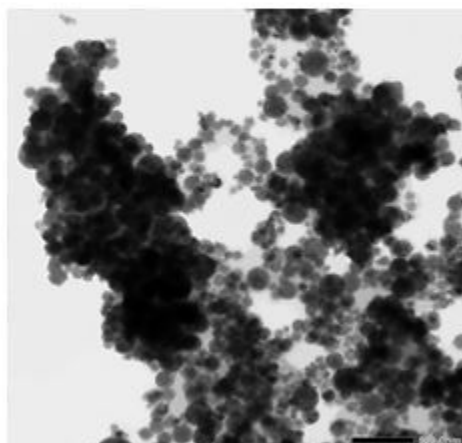
(c)



(d)



(e)



(f)

Figure 13

TEM micrographs of Al₂O₃ nanoparticles dispersed in PAO6 under 20 kHz, 70% amplitude. (a-c-e) For 0.005wt%, 0.01wt% and 0.02wt% NPs after preparation and (b-d-f) For 0.005wt%, 0.01wt% and 0.02wt% NPs after 160 days.

Supplementary Files

This is a list of supplementary files associated with this preprint. Click to download.

- [supplement1.tif](#)